FACTORS EFFECTING THE FATIGUE STRENGTH OF FERRO-CEMENT

David P. Sargent

NAVAL POSTGRADUATE SCHOOL
Monterey, California

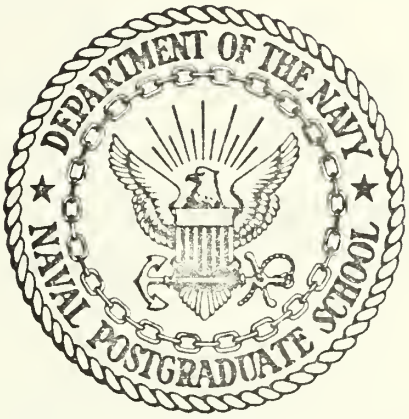

THESIS

FACTORS EFFECTING THE FATIGUE STRENGTH
OF FERRO-CEMENT

by

David P. Sargent, Jr.

December 1974

Thesis Advisor: E. A. McKinnon

Approved for public release; distribution unlimited.

SECURITY CLASSIFICATION OF THIS PAGE (When Data Entered)

REPORT DOCUMENTATION PAGE

READ INSTRUCTIONS BEFORE COMPLETING FORM

1. REPORT NUMBER	2. GOVT ACCESSION NO. / 3. RECIPIENT'S CATALOG NUMBER
4. TITLE (and Subtitle): FACTORS EFFECTING THE FATIGUE STRENGTH OF FERRO-CEMENT	5. TYPE OF REPORT & PERIOD COVERED: Master's Thesis: December 1974
	6. PERFORMING ORG. REPORT NUMBER
7. AUTHOR(s): David P. Sargent, Jr.	8. CONTRACT OR GRANT NUMBER(s)
9. PERFORMING ORGANIZATION NAME AND ADDRESS: Naval Postgraduate School, Monterey, California 93940	10. PROGRAM ELEMENT, PROJECT, TASK AREA & WORK UNIT NUMBERS
11. CONTROLLING OFFICE NAME AND ADDRESS: Naval Postgraduate School, Monterey, California 93940	12. REPORT DATE: December 1974
	13. NUMBER OF PAGES
14. MONITORING AGENCY NAME & ADDRESS (if different from Controlling Office): Naval Postgraduate School, Monterey, California 93940	15. SECURITY CLASS. (of this report): Unclassified
	15a. DECLASSIFICATION/DOWNGRADING SCHEDULE

16. DISTRIBUTION STATEMENT (of this Report)

Approved for public release; distribution unlimited.

17. DISTRIBUTION STATEMENT (of the abstract entered in Block 20, if different from Report)

18. SUPPLEMENTARY NOTES

19. KEY WORDS (Continue on reverse side if necessary and identify by block number)

ferro-cement
fatigue
wire orientation
void sensitivity

20. ABSTRACT (Continue on reverse side if necessary and identify by block number)

Ferro-cement is a composite material consisting of multiple layers of wire mesh impregnated with a cement mortar. Steel rods may be sandwiched in the center to give added strength, and to shape the mesh before application of the mortar. Selection of materials can vary considerably. Investigation of the influence of wire orientation on the fatigue strength of ferro-cement was undertaken in this study. Tests were also conducted to determine the effect on fatigue life of voids in the specimens caused by poor penetration of the mortar.

DD FORM 1 JAN 73 1473 EDITION OF 1 NOV 65 IS OBSOLETE
S/N 0102-014-6601
(Page 1)

SECURITY CLASSIFICATION OF THIS PAGE (When Data Entered)

FACTORS EFFECTING THE FATIGUE STRENGTH OF FERRO-CEMENT

by

David P. Sargent, Jr.
Lieutenant, United States Navy
B.S., Cornell University, 1967

Submitted in partial fulfillment of the
requirements for the degree of

MASTER OF SCIENCE IN MECHANICAL ENGINEERING

ABSTRACT

Ferro-cement is a composite material consisting of multiple layers of wire mesh impregnated with a cement mortar. Steel rods may be sandwiched in the center to give added strength, and to shape the mesh before application of the mortar. Selection of materials can vary considerably. Investigation of the influence of wire orientation on the fatigue strength of ferro-cement was undertaken in this study. Tests were also conducted to determine the effect on fatigue life of voids in the specimens caused by poor penetration of the mortar.

TABLE OF CONTENTS

I. INTRODUCTION ---------- 12

II. BACKGROUND ---------- 13

III. OBJECTIVES OF THIS STUDY ---------- 15

IV. EXPERIMENTAL PROCEDURE ---------- 16

A. GENERAL ---------- 16

B. REINFORCING WIRE ---------- 16

C. SPECIMEN IDENTIFICATION ---------- 17

D. FORMS ---------- 17

E. MORTAR ---------- 18

F. CURING ---------- 19

G. CUTTING SPECIMENS ---------- 19

V. FATIGUE TESTS ---------- 20

A. PURPOSE ---------- 20

B. SPECIMENS TESTED ---------- 20

C. TESTING APPARATUS ---------- 20

D. RESULTS AND DATA ANALYSIS ---------- 21

E. CONCLUSIONS ---------- 23

VI. MONOTONIC BENDING TESTS ---------- 24

A. PURPOSE ---------- 24

B. SPECIMENS TESTED ---------- 24

C. DESCRIPTION OF TESTING APPARATUS ---------- 24

D. RESULTS AND DATA ANALYSIS ---------- 25

E. CONCLUSIONS ---------- 26

VII. TENSILE TESTS ---------- 27

A. PURPOSE ---------- 27

B. SPECIMENS TESTED ---------- 27

C. DESCRIPTION OF TESTING APPARATUS ---------- 27
D. RESULTS AND DATA ANALYSIS ---------- 28
E. CONCLUSIONS ---------- 29
VIII. NOTCH SENSITIVITY TESTS ---------- 30
A. PURPOSE ---------- 30
B. SPECIMEN PREPARATION ---------- 30
C. TESTING ---------- 32
D. RESULTS AND DATA ANALYSIS ---------- 32
E. CONCLUSIONS ---------- 34
IX. CONCLUSIONS AND RECOMMENDATIONS ---------- 35
A. CONCLUSIONS ---------- 35
B. RECOMMENDATIONS ---------- 36
APPENDIX A DEFINITIONS ---------- 37
APPENDIX B CALCULATIONS ---------- 40
APPENDIX C TABLES ---------- 44
APPENDIX D FIGURES ---------- 51
LIST OF REFERENCES ---------- 88
INITIAL DISTRIBUTION LIST ---------- 90

LIST OF TABLES

TABLE

I. List of Specimens and Type of Tests Conducted ---------- 44

II. Mortar Proportions ---------- 45

III. Slump Readings for Different Panels ---------- 45

IV. Monotonic Bending Data ---------- 46

V. Stress Ratios for Different Panel Types ---------- 47

VI. Tensile Test Data ---------- 48

VII. Tensile and Flexural Test Data and Stress Ratios ---------- 49

VIII. Test Data for Panel QGL7S2 ---------- 50

IX. Monotonic Bending Data for Panel QGL7S2 ---------- 50

LIST OF FIGURES

FIGURE

1. Sketch of Shipping Roll ---------- 51
2. Sketch of Wire Orientation for Various Panels ---------- 52
3. Plywood Form With Wire Mesh ---------- 53
4. Specimen Curing Tents ---------- 54
5. Saw for Cutting Specimens from Panels ---------- 55
6. Fatigue Testing Jig ---------- 56
7. Close-Up of Fatigue Failure at Maximum Deflection of Three-Quarters of an Inch ---------- 57
8. S_f-N Plot for Panel QUL7S3, All Layers With Stronger Wires Parallel to Specimen Axis ---------- 58
9. S_f-N Plot for Panel QUA7S1, Both Outer, and Each Alternate Layer With Stronger Wires Parallel to Specimen Axis --------- 59
10. S_f-N Plot for Panel QUB7S1, Both Outer, and Each Alternate Layer With Weaker Wires Parallel to Specimen Axis ---------- 60
11. S_f-N Plot for Panel QUT7S2, All Layers With Weaker Wires Parallel to Specimen Axis, One Side With Outermost Wires Perpendicular to Axis ---------- 61
12. S_f-N Plot for Panel QUA7S1, Cut With Weaker Wires parallel to Specimen Axis, Outermost Wires Perpendicular to Axis -------- 62
13. S_f-N Plot Comparing Results of Panels QUT7S2 and QUB7S1 ----- 63
14. S_f-N Plot Comparing Results for Panels QUT7S2, QUB7S1, and QUA7S1 With Stronger Wires Parallel to Specimen Axis -------- 64
15. Sketch of Monotonic Bending Scheme ---------- 65
16. Monotonic Bending Jig ---------- 66
17. Monotonic Bending Stress vs. Deflection Plot for Panel QUA7S1 ---------- 67

18. Monotonic Bending Stress vs. Deflection Plot for Panel QUT7S2 ---------- 68

19. Monotonic Bending Stress vs. Deflection Plot for Panel QUT7S2 ---------- 69

20. Monotonic Bending Stress vs. Deflection Plot for Panel QUL7S3 ---------- 70

21. Monotonic Bending Stress vs. Deflection Plot for Panel QUA7S1 ---------- 71

22. Monotonic Bending Stress vs. Deflection Plot for Panel QUB7S1 ---------- 72

23. Epoxy Coating on Tensile Specimen ---------- 73

24. Tensile Failure Along Cleavage Plane Caused by Alignment of Mesh Layers ---------- 74

25. Poorly Impregnated Panel Before Cutting ---------- 75

26. Views of Specimen QGL7S2-11 ---------- 76

27. Views of Specimen QGL7S2-6 ---------- 77

28. Views of Specimen QGL7S2-8 ---------- 78

29. Views of Specimen QGL7S2-4 ---------- 79

30. Edge View of Specimen QGL7S2-4 Showing Fatigue Crack -------- 80

31. Views of Specimen QGL7S2-5 ---------- 81

32. Views of Specimen QGL7S2-10 ---------- 82

33. Views of Specimen QGL7S2-2 ---------- 83

34. Views of Specimen QGL7S2-7 ---------- 84

35. Views of Specimen QGL7S2-1A ---------- 85

36. Views of Specimen QGL7S2-3 ---------- 86

37. Monotonic Bending Stress vs. Deflection Plot for Panel QGL7S2 ---------- 87

TABLE OF SYMBOLS AND ABBREVIATIONS

SYMBOLS

S_f	Maximum Cyclic Flexural Stress
S_y	Monotonic Bending Yield Stress
S_u	Monotonic Bending Ultimate Stress
S_t	Tensile Ultimate Stress
S	Stress
N	Number of Cycles to Fatigue Failure
MB	Monotonic Bending
F	Fatigue Testing
T	Tensile Testing

ABBREVIATIONS

psi	Pounds-Force per Square Inch
in	Inch
lbf	Pounds-Force
cm	Centimeter

ACKNOWLEDGEMENT

Research for this study was conducted utilizing the facilities of the Mechanical Engineering Department at the Naval Postgraduate School, Monterey, California. The technical expertise and willing assistance of the technicians in the Mechanical Engineering Department were of great value throughout this study.

Acknowledgement is due:

Dr. Kenneth Saczalski and the Office of Naval Research, for supporting this study;

Pat Holmes, for the time and labor she dedicated in typing this report.

Special appreciation goes to Professor Edwin A. McKinnon, the author's advisor, for encouragement, guidance, and generous contribution of time.

This thesis is dedicated to my wife, Janet, for her patience and assistance during the research for, and preparation of, this report.

I. INTRODUCTION

Ferro-cement is a composite material consisting of multiple layers of wire mesh impregnated with a cement mortar. Steel rods may be sandwiched in the center to give added strength and to shape the mesh before application of the mortar. The type of wire mesh and mortar used vary depending on the intended use, cost, availability, and personal whim of the designer.

Ferro-cement has some unique properties such as flexibility, formability and good fatigue characteristics. These properties have not been fully investigated and catalogued. Fatigue properties have received the least amount of attention to date. Simpson [1][1], who has made the largest contribution to this area, concentrated on investigating the effect of various material compositions on the fatigue strength of ferrocement.

The need for additional insight into the fatigue characteristics motivated this study. Investigations were conducted to determine what effects on fatigue strength were caused by various orientations of the wire in the mesh. Plots and tables of flexure stress versus fatigue life, and corresponding monotonic bending and tensile data were developed.

Additional studies were undertaken to gain insight into the relationship between fatigue life and surface voids caused by poor penetration of the mortar into the wire mesh. Visual comparisons of specimens before and after fatigue failure were the primary type of data collected. The effect of filling the voids with epoxy was also explored.

---

[1]Numbers in parentheses identify references; see pages 88-89.

II. BACKGROUND

The initial development of ferro-cement is credited to the Frenchman Jean Louis Lambot [2] who in 1848 used ferro-cement to make a boat hull. Although numerous applications of the material can be cited dating from its initial development [3,4,5], the true utility and attractiveness of ferro-cement has been recognized only in the past ten years. Suitability for construction of fishing boats and pleasure craft provided the impetus for the rekindled interest. New Zealand, England, and Canada were pioneers in ferro-cement boat building [6,7,8,9]. Experience gained through these maritime applications led to a better understanding of the potential of ferro-cement as a construction material for a variety of uses. Extreme durability, minimum maintenance, low cost materials, and almost unlimited formability make ferro-cement an attractive building material. Some current applications of ferro-cement are discussed by Simpson [1] and Haynes [10].

As recognition of the advantages of ferro-cement increased, need for standardization of the material and its physical and mechanical properties became obvious. The available data on reinforced concrete is not applicable. Ferro-cement is not reinforced concrete, but a composite material which demonstrates unique properties superior to either the wire mesh or mortar alone. Bezukladov [5] differentiates between reinforced concrete and ferro-cement in terms of the ratio of surface area of reinforcement to the volume of the composite. For a specific surface K (Appendix A, part 1) of approximately 2 cm^{-1}, the material is classified as ferro-cement and for a specific surface less than 0.5 cm^{-1} it is classified as reinforced concrete. Recognition that ferro-cement does

act differently from reinforced concrete has resulted in extensive testing. Many of the tests have involved specialized investigation to determine the acceptability of a structure already built, or of one proposed. Other systematic testing has been done, but involved primarily monotonic testing methods [6,7,8,9]. The immense variety of materials, fabrication techniques, types of mortar, and curing methods available renders standardization of ferro-cement and corrosponding testing procedures extremely difficult. Brauer [3] and Simpson [1] detail many of the methods and materials currently in use.

With the increased interest in ferro-cement since about 1966, more extensive and standardized fabrication and testing have been conducted. References [6,7,8,9] provide details of these advances. Simpson [1] undertook the first extensive standardized fatigue testing to form a data base of the effect that material selection has on fatigue life and fatigue fracture mechanisms. His results included comparison with monotonic test data.

III. OBJECTIVES OF THIS STUDY

Based on the data and conclusions of Simpson [1]) and Brauer [3], the three factors effecting both monotonic and fatigue strength of ferro-cement are selection of materials, fabrication technique, and curing methods.

Simpson [1] determined that ungalvanized, welded wire mesh was stronger than galvanized mesh. Because of the method used to weld the wires together to form a mesh the tensile strength of the wires across the mesh were lower than in the direction of the wire as unrolled. In Simpson's [1] study specimens were prepared with all layers of wire having the stronger direction along the axis of the test specimen. Simpson [1] and Keeton [11] also determined that certain types of cement gave superior strength and that water curing resulted in stronger specimens than steam curing.

This study was designed to expand the data on fatigue strength. Specimens similar to Simpson's [1] were fabricated using Portland Type II cement. The influence of wire orientation on the fatigue strength of ferro-cement was studied in this investigation.

A separate study was conducted to determine the effect on fatigue life of voids in the test specimens caused by poor penetration of mortar. Comparing results of tests on samples with voids to those on samples with voids filled with epoxy provided insight into the notch sensitivity of ferro-cement.

IV. EXPERIMENTAL PROCEDURE

A. GENERAL

All ferro-cement specimens were prepared in the same manner to insure maximum uniformity. Individual specimens measured approximately 2 3/4 inches wide, 1/2 inches thick, and 18 inches long. These samples were cut from panels measuring 36 by 18 by 1/2 inches. Four basic variations in wire orientation were chosen. Mortar composition, layup procedure, and curing method were identical for each of the four configurations.

B. REINFORCING WIRE

Ungalvanized, one-half inch, welded, square wire mesh was chosen for reinforcement since it had proven superior in strength in Simpson's [1] study. The individual wires were 0.040 inches in diameter. Tensile testing of the mesh showed an ultimate strength of approximately 150,000 psi in the long direction of the mesh as unrolled from the shipping roll (36 inches wide by 50 feet long), and 114,000 psi in the transverse direction. Preparation of the wire included cutting to approximately 18 by 36 inches, boiling in a solution of 5 pounds of trisodium phosphate in 25 gallons of water to remove any oil, and flattening with sheet metal rolls prior to mounting on the forms. Variations in wire orientation were accomplished by cutting the 18 by 36 inch pieces in two possible ways; Type I, with the 36 inch direction perpendicular to the long axis of the wire as unrolled from the shipping roll; and Type II, with the 36 inch direction parallel to the long axis of the wire as shown in Fig. 1.

C. SPECIMEN IDENTIFICATION

An identification system for each 18 inch by 36 inch ferro-cement panel and specimen cut from it was chosen to identify the test specimens. Appendix A, part 1 details the specimen identification system.

All samples in this part of the study were steam cured and fabricated using Portland Type II cement and seven layers of ungalvanized wire mesh. Sketches illustrating the wire orientation in each of the basic panels used in this study is given in Fig. 2. Their identification numbers are QUL7S3, QUT7S2, QUA7S1, and QUB7S1. Table I lists all specimens prepared from these panels, and the type of test conducted.

D. FORMS

Forms for fabricating the 18 inch by 36 inch panels were constructed from 3/4 inch exterior plywood cut to approximately 20 inches by 40 inches. To prevent warping and accompanying distortion of the ferro-cement panel, the plywood was reinforced with a frame of 2 inch by 4 inch fir. A sheet of plastic was stretched over the plywood to provide a smooth vapor barrier between the mortar and plywood. Seven layers of wire mesh were then stapled to the frames. The first layer was mounted with the outermost wires parallel to the 18 inch direction, thus resulting in the outermost wires being parallel to the long axis of the 2 3/4 inch by 18 inch test specimens. Three subsequent layers also had the 18 inch direction wires down and the last three layers had them facing up. Each layer was staggered to give uniform distribution of the reinforcement throughout the panel. In panel number QUT7S2, an error was made in attaching the seventh layer, resulting in the 36 inch wires being out. Thus, all 2 3/4 inch by 18 inch specimens from that panel have

outer wires on one side parallel to the long axis and those on the other side transverse. The influence of this is discussed in Chapter V. Wooden strips were nailed around the edges of the plywood to give a panel thickness just sufficient to cover the outer wires. Small holes were drilled in several places in the backing plywood and fine stainless steel wire was used to tie the layers of mesh tightly against the form. These wires were easily cut from the back of the plywood after curing. Figure 3 shows a completed form prior to mortaring.

E. MORTAR

Although Simpson [1] used an expansive cement and Type V Portland cement; Type II Portland cement was chosen for this study because of its greater availability and longer shelf life. The mortar contained washed and dried beach sand, pozzolan for added fines, and a 0.45 water to cement ratio. Because the sand was furnace dried prior to use, additional water was added (1% of the weight of the sand). Although the mesh was ungalvanized, 300 parts per million by weight of chromium trioxide were added to the water as recommended by Christensen and Williamson [12] to ensure against gas production from electrolytic cell action. The mortar was mixed manually in approximately 70 pound batches. Exact proportions are given in Table II. Weights were controlled to within 0.05 pounds. The forms and wheelbarrow were dampened prior to mixing and layup to prevent excessive water absorption. Slump tests on the mortar are given in Table III. Each batch was sufficient for 2 panels plus a 4 inch compression cylinder. Panels QUA7S1 and QUB7S1 were mortared with one batch and panels QUL7S3 and QUT7S2 were mortared from another. To ensure adequate penetration, the mortar was worked into the mesh with a trowel,

the forms were bounced several times on a concrete floor and a pencil vibrator was used. Panel QGL7S2 used in the notch sensitivity tests, Chapter VIII, was prepared from a separate but similar batch.

F. CURING

Steam curing was chosen for this study. The mortared panels were placed in the curing tent shown in Fig. 4 about 12 hours after mortaring. The temperature was brought from ambient to 160°F gradually over a 4 hour period. The 160°F temperature was maintained for 18 hours and then gradually reduced to ambient over a 4 hour period. All panels, except QGL7S2, discussed in Chapter VIII, were cured at the same time.

G. CUTTING SPECIMENS

Each panel was cut using the saw shown in Fig. 5 which had a diamond impregnated carbide blade. Except for QUA7S1, the cuts were all made parallel to the 18 inch direction. Panel QUA7S1 had 7 samples cut from it parallel to the 18 inch axis and 6 cut parallel to the 36 inch axis. This yielded some samples with the outer wires parallel to the long axis and some with the outer wires perpendicular to the long axis.

V. FATIGUE TESTS

A. PURPOSE

One of the purposes of this study was to compare the fatigue life of specimens with varying wire orientations. Because of the large number of samples required to construct a complete flexural stress vs. fatigue life (S_f-N) curve, it was decided to test six samples from each of the four variations; three at a relatively high stress level and three at a relatively low stress level. This would give the slope of the S_f-N curve and a feeling for the scatter in the data, but would not provide an endurance limit. Stress levels were chosen based on data from Simpson's [1] work.

B. SPECIMENS TESTED

Six specimens were chosen from each of the panels QUB7S1, QUL7S3, and QUT7S2. Additionally, six were chosen from QUA7S1 with the outer wires oriented parallel to the long axis and three with the outer wires transverse to the long axis. As noted in Chapter IV, the specimens from panel QUT7S2 had the outer wires on one side parallel to the long axis and on the other side transverse.

C. TESTING APPARATUS

Specimens were mounted on a Baldwin Locomotive Works, Sonntag Model SF-1U fatigue testing machine using the jig pictured in Fig. 6. Any initial preload was removed and specimens were cycled in load control at 30 hertz. The specimens were measured and the load required for the desired stress levels of 1,300 psi and 1,750 psi were calculated as shown in Appendix B, part 1. The applied load could be set to within 0.5 pounds.

The loading thus obtained was a sinusoidally varying moment of equal magnitude over the eight inch center section of the specimen. Failure criteria was defined to be a total deflection of one-half inch. Micro switches were set to stop the machine when this deflection was reached. The cycle counter recorded the number of completed cycles to the last thousand. After several specimens had failed under the one-half inch criterion, the micro switches were readjusted to give a deflection in excess of three-quarters of an inch to determine how many additional cycles could be expected. In each case the new maximum deflection and specimen failure was reached in less than one thousand additional cycles. Failure at three-quarters of an inch deflection was accompanied by some mortar being thrown out and several wires breaking, Fig. 7. The one-half inch total deflection criterion was used for all subsequent specimens.

D. RESULTS AND DATA ANALYSIS

After determining the number of cycles to failure, each specimen was inspected. In most cases, there was one visible crack where failure was concentrated and in only a few cases was mortar thrown off, with no broken wires observed on any of the samples. The specimens were measured for width and thickness to the nearest 0.02 inches adjacent to the area of failure. These measurements and the applied load were used to determine the failure stress and the uncertainty in the measurements by calculations shown in Appendix B, parts 1 and 5. A digital computer program was utilized for these calculations and for obtaining a first-order least squares fit of the data points. Plots of the resulting S_f-N curves are given in Figs. 8-12 with uncertainty bars shown. There

is one S_f-N curve for each of panels QUB7S1, QUT7S2, and QUL7S3. Two curves are presented for panel QUA7S1; one for specimens with the outer wires parallel to the specimens' long axis and one for those with the outer wires in a transverse direction. It was anticipated that specimens with the strongest direction of all layers of the wire mesh aligned with the axis of the specimens would give the longest life at a given stress. These would be specimens QUL7S3-1 through QUL7S3-6. Next strongest were expected to be those from panel QUA7S1 with the outer layers having the strongest wires parallel to specimen axis, and interior layers alternating. Specimens QUA7S1-1 through QUA7S1-6 are included in this group. Third strongest were expected to be QUB7S1-1 through QUB7S1-6 with alternating wire layers, but with outer layers having the weaker wires parallel to the axis. Fourth strongest should be the unsymmetrical specimens (1 through 6) from panel QUT7S2. These have the strongest wires outermost and axial on one side and the weaker wires outermost and transverse on the other. The weakest configuration was expected to be the three QUA7S1 samples with the stronger wires outermost but transverse to the specimen axis on both sides. Included in this group were QUA7S1-7, 9, 10.

These expectations were borne out very well during testing, except that the QUB7S1 and QUT7S2 configurations yielded virtually similar results. This is demonstrated in Fig. 13. Also, although the QUA7S1 specimens sustained more cycles at the high stress level, the life of the QUA7S1, QUB7S1, and QUT7S1 panels at the 1,300 psi stress level were essentially equal. Figure 14 shows these three S_f-N curves superimposed.

Failure of the fatigue specimens in this study differed from previous specimens (Simpson's investigation [1]) observed by the author in that very little mortar was thrown out upon failure. This difference was attributed to fabrication procedure. Previous samples had a layer of unreinforced mortar one-sixteenth of an inch thick on top of the layers of wire. The samples in this study had the outer layers of wire just covered to prevent corrosion. The thickness of unreinforced mortar was thus on the order of one-hundredth of an inch.

E. CONCLUSIONS

The S_f-N curves developed for the various wire orientations were consistent with expected trends. They substantiated the prediction that the wire strength is the fundamental parameter that determines the fatigue life of the ferro-cement. The failure criterion of one-half inch total deflection produced failure with only minor cracking visible. Since ferro-cement is used for boats and other containers requiring water tight integrity, this aspect is important. Although seepage might occur through these cracks, catastrophic rupture would not be likely. This conclusion was supported by the remaining tensile strength after fatigue failure. This aspect is discussed in Chapter VII. The relatively small scatter in the fatigue data demonstrated very good uniformity of the test specimens from each panel.

VI. MONOTONIC BENDING TESTS

A. PURPOSE

The S_f-N curves developed in the Fatigue Tests were generated from data taken at two stress levels. Monotonic bending tests were conducted to supplement this data by providing stress vs. deflection curves, and also to enable comparison of the monotonic ultimate and yield strengths of the various wire orientations. Additionally, it was desired to visually compare the failure under monotonic loading to that caused by fatigue.

B. SPECIMENS TESTED

To provide some measurement of scatter in the data collected, two similar specimens of each type were tested where possible. A total of nine specimens were tested from the various wire orientations selected as follows: two each from panels QUL7S3 and QUB7S1; four from panel QUT7S2, two with the transverse outer wires on the outside of the bend, and two with the axial outer wires on the outside of the bend; and one from the QUA7S1 panel with the outer wires transverse to the axis.

C. DESCRIPTION OF TESTING APPARATUS

Specimens were loaded in pure bending by means of the arrangement shown in Figs. 15 and 16. The loading rate was approximately 150 pounds per minute. Deflection was measured at the center of the specimen every 0.050 inches by means of dial indicator. Loading was continued until the specimen yielded. The failed specimen was then inspected and measured at the point of failure, with measurements accurate to 0.02 inches. Flexural

bending stress in the specimens with accompanying uncertainty analysis was calculated using simple flexure theory of beams as demonstrated in Appendix B, parts 2 and 6.

D. RESULTS AND DATA ANALYSIS

Uniformity of the test specimens was further substantiated by the minimal scatter in the monotonic bending data. Figures 17-22 are graphs of flexural stress vs. deflection for each type of specimen tested. The uppermost point on these curves indicate the ultimate strength and the starred point (★) represents the flexural yield strength. The definition of yield strength used is that defined by Simpson [1] in his study, namely the point on the curve where the tangent modulus equals the secant modulus at ultimate strength. Table IV lists the various specimens subjected to monotonic flexure testing with their yield and ultimate strengths, and fatigue strength at $N = 10^6$ cycles. Table V gives ratios of yield strength to ultimate strength, flexural strength at 10^6 cycles to ultimate monotonic stress, and fatigue strength at 10^6 cycles to monotonic yield strength, based on the average values of each specimen type. The ratio of yield strength to ultimate strength for all of these specimen types is very nearly 75 percent for each of the specimens tested. This is in good agreement with data from previous studies [9] and [12]. The ratios of fatigue strength at 10^6 cycles to monotonic yield strength, and fatigue strength at 10^6 cycles to monotonic ultimate strength show the same strength gradation among the various wire orientation as was determined by fatigue tests with the exception of the QUA7S1 panel. Data from that panel is inconsistent with the relative strengths observed in fatigue testing. Random scatter is one possible

explanation for this. As noted earlier, this panel was cut two different ways giving some specimens with the outer wires transverse to the axis of the specimen and others wihh the outer wires parallel to the specimen axis. Only one of each type was subjected to monotonic bending. The specimen with the outer wires parallel to the specimen axis fell lowest in the relative monotonic strength ratios and the specimen with the outer wires transverse was near the top of the listing. The fatigue testing showed just the opposite for these wire orientations.

E. CONCLUSIONS

Monotonic bending data was consistent with previous studies in showing a fairly constant ratio of monotonic yield strength to ultimate strength. Other ratios of fatigue strength at 10^6 cycles to monotonic yield strength and fatigue strength at 10^6 cycles to monotonic ultimate strength were in general agreement with the relative strengths of the various wire orientations obtained from fatigue testing.

VII. TENSILE TESTS

A. PURPOSE

Tensile testing of specimens was considered desirable in this study to provide further comparative analysis of the effects of wire orientation, and to provide a base for comparison with other investigations. Because ferro-cement is often utilized for water tight structures, tensile strength before and after fatigue failure is an important parameter to consider in design.

B. SPECIMENS TESTED

As in the monotonic bending tests, two similar specimens from the various panels were selected to get a feeling for the scatter present in the data. For panels QUL7S3, QUT7S2, and QUB7S1, two unfatigued specimens and two fatigued specimens were selected. For panel QUA7S1, two fatigued samples and one unfatigued with the outer wires parallel to the axis were selected as well as two unfatigued samples with the outer wires transverse to the specimen axis.

To ensure proper gripping of the specimens in the testing machine it was necessary to coat the ends of the specimens. Two materials were used with success. One was a two component, epoxy adhesive material, and the other was a two component, polyester automotive body filler material. An example is given in Fig. 23

C. DESCRIPTION OF TESTING APPARATUS

An Universal tensile testing machine was utilized. Each specimen was gripped in serrated jaws. A tensile load was applied at a rate of

approximately 1,000 pounds per minute until the specimen yielded and the load began to decrease. The maximum load was recorded. Upon removal from the test machine, the specimen was measured at the point of yielding and the ultimate tensile stress and associated uncertainty was calculated as demonstrated in Appendix B, parts 3 and 7.

D. RESULTS AND DATA ANALYSIS

The results of the tensile testing are given in Table VI. Comparison of the average ultimate stress before fatigue failure with that after showed a percentage reduction as noted in this table. Although the fatigued specimens demonstrated reduced ultimate strength, the remaining strength ranged from 27 percent to 54 percent of their average, unfatigued ultimate strength. Table VII presents the tensile test data for the various wire orientations and ratios of tensile strength to monotonic ultimate strength, monotonic yield strength, and fatigue strength at 10^6 cycles. The ratios of tensile strength to ultimate strength and tensile strength to yield strength show the same relative values among the wire orientations as those determined from fatigue testing and monotonic bending except that specimens from panel QUA7S1 are again inconsistent with fatigue data. Data from the tensile tests shows greater scatter between similar specimens than was observed in other types of tests. This can be seen by comparing the values of ultimate tensile stress for similar samples listed in Table VI. This scatter was not surprising because of the cleavage planes caused when several layers of mesh had wires joints nearly on top of one another. These areas were weak because the joints are the weakest part of the mesh. Figure 24 is

an example of a tensile failure along one of these planes. These planes were impossible to prevent when fabricating panels because of the irregularity of the mesh. For this reason, tensile testing data was considered to be the least reliable.

E. CONCLUSIONS

Tensile tests showed an overall reduction in ultimate tensile strength between unfatigued and fatigued specimens. Remaining strength after fatigue ranged from 27 to 54 percent of unfatigued strength.

Variations in wire orientation resulted in the same general relative strength standings under tensile testing as those obtained by fatigue and monotonic bending with the exception of specimens from one panel. The data from tensile tests had greater scatter than from the other type tests and was more sensitive to mesh arrangement. Consequently, tensile testing was considered to produce the least reliable data.

VIII. NOTCH SENSITIVITY TESTS

A. PURPOSE

Complete penetration of the mortar through the wire mesh is hard to ensure, particularly in ferro-cement that is fabricated on a form which exposes only one side of the mesh. When poor penetration does occur, it most likely will not be discovered until after curing and, in the case of interior voids, may never be discovered. Because of the time and material expended in the fabrication, a decision must be made whether the material may be used with the voids, may be repaired in some manner, or must be discarded. In order to gain some data on which to base these decisions, specimens were prepared from an 18 inch by 36 inch panel of ferro-cement in which there were many voids. A method of filling the voids was devised and the specimens were subjected to fatigue testing, with and without voids filled, as well as monotonic bending, without voids filled.

B. SPECIMEN PREPARATION

Specimens for these tests were approximately 2 3/4 by 18 by 1/2 inches, and were cut from a panel 18 inches by 36 inches utilizing the saw shown in Fig. 5. The panel used had been fabricated for some previously planned testing, but upon completion of curing, was found to have many surface and interior voids. Figure 25 shows the porous side of panel QGL7S2 prior to cutting. This panel was fabricated using 7 layers of galvanized one-half inch wire mesh. Each layer had the stronger direction of the mesh aligned with the long axis of the specimens. The mortar used was the same proportions as that given in Table II,

and the panel was steam cured for 26 hours. Neither the forms nor the mixing container were wetted prior to mortaring, and a pencil vibrator was the only method used to enhance penetration. These factors are believed to be the cause of the poor penetration.

In cutting the specimens from the panel, an attempt was made to get two that were free of surface voids for control specimens. After cutting, however, some interior voids were found. Eight others were cut and an eight inch section marked in a manner that would prevent having voids adjacent to the clamps on the fatigue testing machine. In an attempt to quantify the extent of voids in each sample, all voids were measured for estimated depth and diameter, and the total volume of voids was calculated. Voids were treated either as cylinders or rectangular parallelepipeds depending on their surface appearance. The total void volume was divided by the volume of the eight inch test section to obtain percentage voids. Details of each specimen and the percentage voids are presented in Table VIII.

The eight specimens with voids were divided into two groups. One group was selected for patching. Filling of voids in the ferro-cement with mortar seemed impossible. Epoxy resin with sand is mentioned by Brauer [3] as satisfactory for sealing joints between panels of ferro-cement. This method was also discarded because of the difficulty in filling the small voids. It was felt that the main objective for void filling should be protection of the wire mesh from corrosion. A two component, epoxy glue was selected. Its fluidity made filling of voids with a small probe possible and its hardness and durability after curing were impressive. Some reduction in notch sensitivity was anticipated for these patched specimens.

C. TESTING

Fatigue testing was the primary means used to compare the unpatched specimens to the patched specimens. Of particular interest was visual inspection to determine where failure occurred, whether voids acted as stress raisers, and whether the epoxy filling made any apparent difference in the location of failures or the fatigue life.

The same fatigue testing machine described in Chapter V was used. Loads were selected to give approximately 1300 psi maximum flexural stress. Actual stress was calculated after failure from measurement of the specimens at the failure crack. One-half inch total deflection was used as the failure criterion.

Two unpatched and unfatigued specimens were also subjected to monotonic bending to provide additional data and to further investigate the effect of voids as stress raisers.

D. RESULTS AND DATA ANALYSIS

Table VIII gives comparative data for the eight fatigue specimens. The randomness of the voids made direct comparison between an unpatched and a patched specimen with the same percentage voids impossible. It appeared, in general, that the specimens with the voids filled demonstrated longer fatigue life. Qualitative comparison of stress and fatigue life data was admittedly chancy and was of secondary importance.

Visual inspection and comparison of the fatigue and bending failures gave good insight into the effect that the surface and interior voids had on the ferro-cement strength. In Fig. 26, visual comparison is made between an unpatched specimen with no surface voids before and after fatigue testing. Figure 26 also gives a closeup of the failure area.

It was expected that surface voids would act as stress concentration points and would thus be the initiation site for fatigue cracks. Inspection of the fatigued specimens suggested that the ferro-cement is not particularly sensitive to voids. As shown in Fig. 27, failure occurred not along the line which joined four moderately sized voids, but in fact occurred nearly where no voids were present. In Fig. 28, the failure crack did pass near two voids, but this failure crack was located about one and one-half inches from the center of the eight inch test section. There was a row of four voids at the center where maximum deflection occurred. Figures 29 and 30 show a specimen with no visible surface voids, but several sizeable voids visible from the edge and near the neutral axis. The failure crack in this specimen passed along the edge of the void, but did not appear to originate at the void.

Visual inspection of the specimens with epoxy filled voids provided more interesting data. As inspection of Figs. 31 and 32 shows, failure of these two specimens was well distributed despite the presence of several epoxy filled voids. Failure of specimens in Figs. 33 and 34 again was fairly well distributed, and was not concentrated at voids.

This distributed nature of the failure cracks, and the generally higher fatigue life of the epoxy patched specimens suggested that the unfilled voids did hasten failure once it originated, and that the epoxy patching reduced this tendency.

Monotonic bending of two specimens was done with the sides containing voids on the inside of the curvature. Comparison of these samples before and after yielding is given in Figs. 35 and 36. Table IX gives

values of yield and ultimate strengths. Both specimens deformed uniformly and the voids had no apparent effect. Insufficient samples were available to monotonically bend any with the imperfect side outward to the bend, or to monotonically test any with epoxy filled voids.

Stress vs. deflection curves are presented in Fig. 37 for the monotonically failed specimens. These curves are the same general shape, but with lower ultimate strength as those presented in Chapter VI. The lower strength was expected, as the galvanized wire mesh had a lower yield than the ungalvanized mesh used in the specimens of Chapter VI. These stress deflection curves suggested little notch sensitivity.

E. CONCLUSIONS

Visual inspection of the poorly impregnated specimens suggested that the voids would act as stress concentrations and thus act as initiation sites for fatigue cracks. Short life was thus expected. Observed data, although limited to ten specimens, suggested that the ferro-cement was not particularly void sensitive. Fatigue crack propagation appeared to be enhanced by adjacent voids after initiation in those specimens without epoxy filled voids. This tendency was reduced by the epoxy filling and longer life was obtained with the patched specimens.

IX. CONCLUSIONS AND RECOMMENDATIONS

A. CONCLUSIONS

As explained in Chapter III the main objectives of this study were to determine the effects on the fatigue strength and monotonic bending and tensile strengths that variations of wire mesh orientations in ferrocement produced. Additionally, the effect of surface and interior voids caused by poor mortar penetration was to be investigated.

Data from this study shows conclusively that wire strength and orientation was a major factor in the fatigue and monotonic strengths. Wire mesh with different strength in two perpendicular directions was used to show that maximum strength was attained by aligning the strongest direction of each layer wire mesh with the long axis of the test specimen. Strength decreased as more layers of the mesh were oriented with the weaker direction parallel to the long axis of the specimen. It was also shown that the outermost wires should be aligned with the axis of the specimen for maximum bending strength. Transverse outer wires produced the weakest configuration.

Keeping the coating of mortar over the outer wires to a minimum thickness reduced the amount of mortar thrown off at failure.

The notch sensitivity tests suggested that fatigue cracks did not initiate at surface voids, but that surface and interior voids did tend to hasten failure once a crack had initiated. Filling of voids with an epoxy glue seemed to significantly reduce this tendency and increased the fatigue life.

B. RECOMMENDATIONS

Further investigation into the effects of arranging some, or all, layers of the mesh at a 45 degree angle to the specimen axis would be appropriate. Also, fatigue testing of larger, square panels of ferro-cement, subjected to biaxial stresses, might reveal more advantageous wire orientation schemes, and provide a measure of the size sensitivity of ferro-cement specimens. Fatigue testing of larger, ferro-cement panels with steel rod reinforcement is also desirable. The area of void sensitivity has barely been touched in this study. Development of a system to better detect and quantify voids, and subsequent extensive testing of representative samples is needed to develop reliable design and acceptance data for ferro-cement. Reference [13] gives many excellent sources for background information for further study.

APPENDIX A DEFINITIONS

1. Calculation of Specific Surface

$$K = \frac{2\pi dn}{at}$$

where,

K = Specific surface

n = Number of layers of mesh

d = Wire diameter (in)

a = Wire spacing (in)

t = Specimen thickness (in)

2. Specimen Identification System

Each test specimen is labelled with a code of the form: $X_1X_2X_3X_4X_5X_6$-X_7

The individual characters have the following meanings:

X_1: Type of cement
- P = Portland Type V
- Q = Portland Type II
- E = Expansive

X_2: Wire Type
- G = Galvanized
- U = Ungalvanized

X_3: Wire Orientation
- L = Longitudinal (Long wires on roll are parallel to long dimension of specimen.)
- T = Transverse (Short wires on roll run parallel to long dimension of specimen.)
- A = Alternating (Layers alternate between L and T; outer layers are L type for odd number of layers.)

B = Alternating (Layers alternate between L and T; outer layers are T orientation for odd number of layers.)

C = Wires run at 45 degree angle to long and short axes of specimen.

N = Used for square panels where T = A.

X_4: Number of layers of wire mesh

X_5: Method of curing S = 26 hour steam cure.
W = 28 day water cure.

X_6: Successive number of panels of this type

X_7: Specimen number; identifies specimen cut from larger panel

EXAMPLE: QUL7S1 identifies a panel (18 x 36 inches)
QUL7S1-10 is the tenth specimen cut from this panel.

APPENDIX B CALCULATIONS

1. Maximum Fatigue Flexure Stress

From the flexure theory of beams:

$$S_f = \frac{Mh}{2I} = \frac{6\,M}{bh^2}$$

$$M = \frac{R\,P}{2} = 3\,P$$

Thus, $$S_f = \frac{18\,P}{b\,h^2}$$

where,

S_f = maximum stress due to flexure (psi)

M = applied bending moment (lbf-in)

P = amplitude of applied cyclic bending force (lbf)

R = fatigue fixture moment arm (6 in)

h = specimen thickness (in)

b = specimen width (in)

I = specimen cross-section moment of inertia (in^4)

2. Monotonic Bending Stress

From flexure theory of beams:

$$S = \frac{M\,h}{2\,I} = \frac{6\,M}{b\,h^2}$$

$$M = \frac{R\,P}{2} = \frac{3\,P}{2} \quad \text{for fixture used}$$

Thus, $$S = \frac{9\,P}{b\,h^2}$$

where,

S = maximum stress due to bending (psi)

M = applied bending moment (lbf-in)

R = monotonic bending fixture moment arm (3 in)

P = total load applied by the test machine (lbf)

h = specimen thickness (in)

b = specimen width (in)

I = specimen cross-section moment of inertia (in^4)

3. Tensile Stress

$$S_t = \frac{P}{b\,h}$$

where,

S_t = ultimate tensile stress (psi)

b = specimen width (in)

h = specimen thickness (in)

P = tensile load applied by machine (lbf)

4. Uncertainty Analyses

Utilizing the second-power equation from Kline and McClintock [14]:

$$\text{error in } X = \left[\sum_{i=1}^{n} \left(\frac{\partial S \omega_i}{\partial x_i} \right)^2 \right]^{\frac{1}{2}}$$

where

$X = X(x_1, x_2, x_3, \ldots x_4)$

ω_i = uncertainty in the measurement of parameter x_i

5. Fatigue Flexure Stress Uncertainty

Uncertainty in S_f:

$$= \left[\left(\frac{18\ \omega_p}{bh^2} \right)^2 + \left(\frac{18\ P\ \omega_b}{b^2h^2} \right)^2 + \left(\frac{36\ P\ \omega_h}{bh^3} \right)^2 \right]^{\frac{1}{2}}$$

using

ω_i = 0.5 lbf = uncertainty in load

ω_b = 0.02 in = uncertainty in specimen width

ω_h = 0.02 in = uncertainty in specimen thickness

Uncertainty in S_f:

$$= \left[\left(\frac{9}{bh^2} \right)^2 + \left(\frac{0.36\ P}{b^2h^2} \right)^2 + \left(\frac{0.72\ P}{bh^3} \right)^2 \right]^{\frac{1}{2}}$$

6. Monotonic Bending Stress Uncertainty

Uncertainty in S:

$$= \left[\left(\frac{9\ \omega_p}{bh^2} \right)^2 + \left(\frac{9\ P\ \omega_b}{b^2h^2} \right)^2 + \left(\frac{18\ P\ \omega_h}{bh^3} \right)^2 \right]^{\frac{1}{2}}$$

using

$\omega_p = 1.0$ lbf

$\omega_b = 0.02$ in

$\omega_h = 0.02$ in

Uncertainty in S:

$$= \left[\left(\frac{9}{bh^2} \right)^2 + \left(\frac{0.18\ P}{b^2h^2} \right)^2 + \left(\frac{0.36\ P}{bh^3} \right)^2 \right]^{\frac{1}{2}}$$

7. Tensile Stress Uncertainty

Uncertainty in S_t:

$$= \left[\left(\frac{\omega_p}{bh} \right)^2 + \left(\frac{P\ \omega_b}{b^2h} \right)^2 + \left(\frac{P\ \omega_h}{bh^2} \right)^2 \right]^{\frac{1}{2}}$$

using

$\omega_p = 1.0$ lbf

$\omega_b = 0.02$ in

$\omega_h = 0.02$ in

Uncertainty in S_t:

$$= \left[\left(\frac{1}{bh} \right)^2 + \left(\frac{.02\ P}{b^2h} \right)^2 + \left(\frac{.02\ P}{bh^2} \right)^2 \right]^{\frac{1}{2}}$$

APPENDIX C TABLES

Table I

List of Specimens and Type of Tests Conducted

Specimen Number	Panel QUL7S3	Panel QUB7S1	Panel QUT7S2	Panel QUA7S1	Panel QGL7S2
1	F&T	F&T	F	F	MB
2	F&T	F&T	F	F	F (with epoxy)
3	F	F	F	F&T	MB
4	F	F	F&T	F	F
5	F	F	F&T	F&T	F (with epoxy)
6	F	F	F	F	F
7	MB	not tested	T	F*	F (with epoxy)
8	MB	not tested	T	MB*	F
9	not tested	MB	MB	F*	no spec.
10	not tested	MB	MB	F*	F (with epoxy)
11	T	T	MB*	T*	F
12	T	T	MB*	T*	no spec.
13				MB	

* Outer wires perpendicular to specimen axis.

Table II

Mortar Proportions

Component	Quantity
Portland Type II Cement	20 lbs.
Pozzolan	1 lb.
Beach Sand (washed, dried, graded)	39 lbs.
Water	9.4 lbs.
Chromium Trioxide	300 ppm by weight of water

Table III

Slump Readings for Different Panels

Panel Number	Mortar Batch	Mortar Slump
QUA7S1	#2	3.3 in.
QUB7S1	#2	3.3 in.
QUL7S3	#3	4.0 in.
QUT7S2	#3	4.0 in.
QGL7S2	#1	1.8 in.

Table IV

Monotonic Bending Data

Specimen Number	S_y		S_u		S_f @ $N=10^6$
	Specimen	Average	Specimen	Average	
QUL7S3-7	3,680	3,688	5,205	5,135	1,375
QUL7S3-8	3,695		5,064		
QUB7S1-9	3,285	3,178	4,355	4,192	1,110
QUB7S1-10	3,070		4,029		
QUT7S2-9	5,475	5,413	7,212	7,083	1,170
QUT7S2-10	5,350		6,954		
QUT7S2-11	4,345	4,623	5,753	6,033	1,170
QUT7S2-12	4,900		6,312		
QUA7S1-8	3,260	3,260	4,458	4,458	1,035
QUA7S1-13	5,225	5,225	7,163	7,163	1,020

Table V

Stress Ratios for Different Panel Types

Specimen Type	S_y/S_u	S_f^*/S_u	S_f/S_y
QUL7S3-7&8	0.718	0.268	0.373
QUB7S1-9&10	0.758	0.265	0.349
QUT7S2-9&10	0.764	0.165	0.216
QUT7S2-11&12	0.766	0.194	0.253
QUA7S1-8	0.731	0.232	0.317
QUA7S1-13	0.729	0.142	0.195

* S_f is the value at $N=10^6$

Table VI

Tensile Test Data

Specimen Number	S_t				Percent Reduction in S_t	Percent Original S_t left
	Before Cycling	Average	After Fatigue	Average		
QUL7S3-11	2,953	3,038				
-12	3,123					
-1			1,821	1,388	45.7%	54.3%
-2			954.6			
QUB7S1-11	2,308	2,195				
-12	2,081					
-1			1,407	1,608	73.7%	26.7%
-2			1,808			
QUT7S2-7	3,023	2,949				
-8	2,874					
-4			1,728	1,732	58.7%	41.3%
-5			1,736			
QUA7S1-11*	2,908	3,058	Not			
-12*	3,208		Tested			
QUA7S1-3**	Not		1,873	1,857		
-5**	Tested		1,840			

* Outer wires transverse to specimen axis; ** Outer wires parallel.

Table VII

Tensile and Flexural Test Data and Stress Ratios

Panel Type	Average S_t	Average S_u	Average S_y	S_f @ $N=10^6$	S_t/S_u	S_t/S_y	S_t/S_f
QUL7S3	3,038	5,135	3,688	1,375	0.592	0.824	2.21
QUB7S1	2,195	4,192	3,178	1,110	0.524	0.691	1.98
QUT7S2*	2,949	7,083	5,463	1,170	0.416	0.540	2.52
QUT7S2**	2,949	6,033	4,623	1,170	0.489	0.638	2.52
QUA7S1***	3,058	4,458	3,260	1,035	0.686	0.938	4.39

* Outermost wires on convex side were parallel to specimen axis during MB.
** Outermost wires on convex side were transverse to specimen axis during MB.
*** Outermost wires on both sides were transverse to specimen axis for all tests.

Table VIII

Test Data for Panel QGL7S2

Speciment Number	Percent Voids	S_f	N @ S_f
QGL7S2-1A	0.09	NA	NA
-2	0.37	1,361	165,000
-3	0.03	NA	NA
-4	0.04	1,509	83,000
-5	0.34	1,569	255,000
-6	0.08	1,385	161,000
-7	0.17	1,385	171,000
-8	0.32	1,439	130,000
-10	0.05	1,456	115,000
-11	0.00	1,328	94,000

Table IX

Monotonic Bending Data for Panel QGL7S2

Specimen Number	S_y	S_u
QGL7S2-1A	4,000	4,622
QGL7S2-3	4,405	5,687

APPENDIX D FIGURES

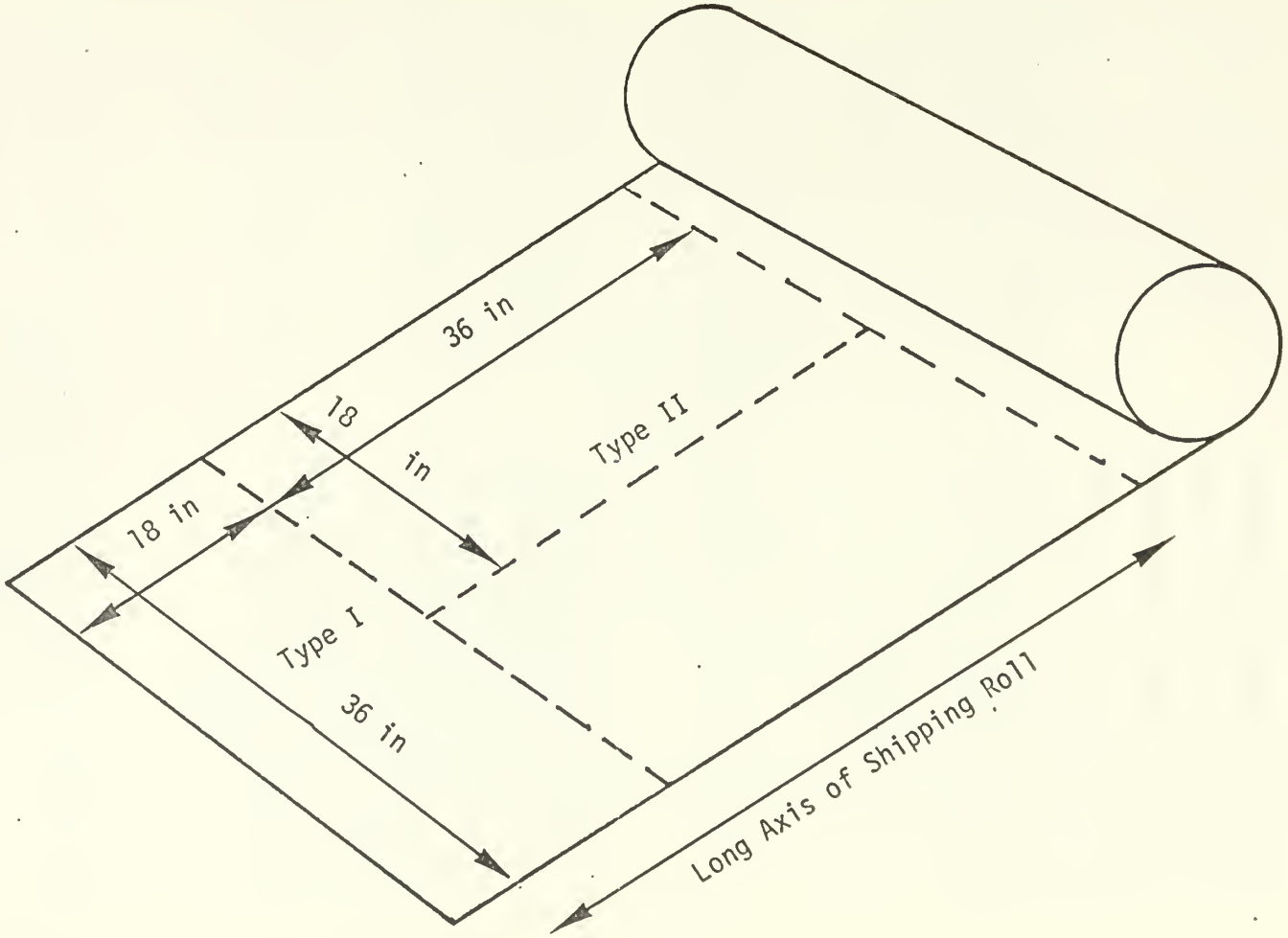

FIGURE 1. Sketch of Shipping Roll

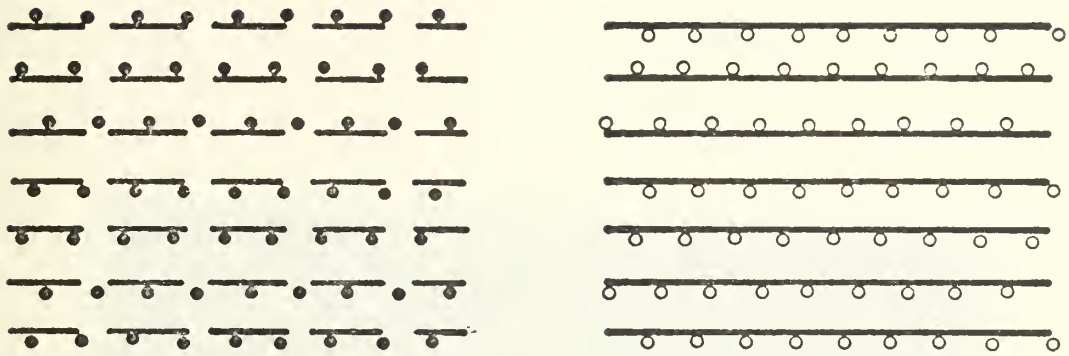

QUL7S3

QUT7S2

36 inch direction of all panels

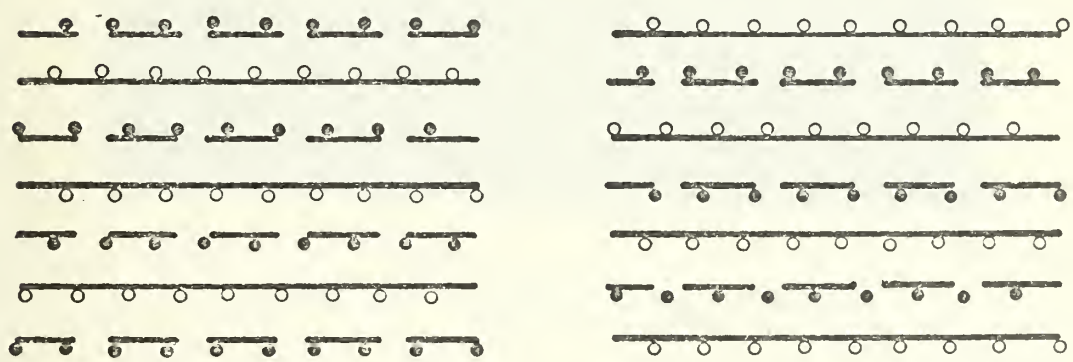

QUA7S1

QUB7S1

o , —— —— —— Represent wires transverse to the long axis of the shipping roll.

• , ———————— Represent wires parallel to the long axis of the shipping roll.

FIGURE 2. Sketch of Wire Orientation for Various Panels

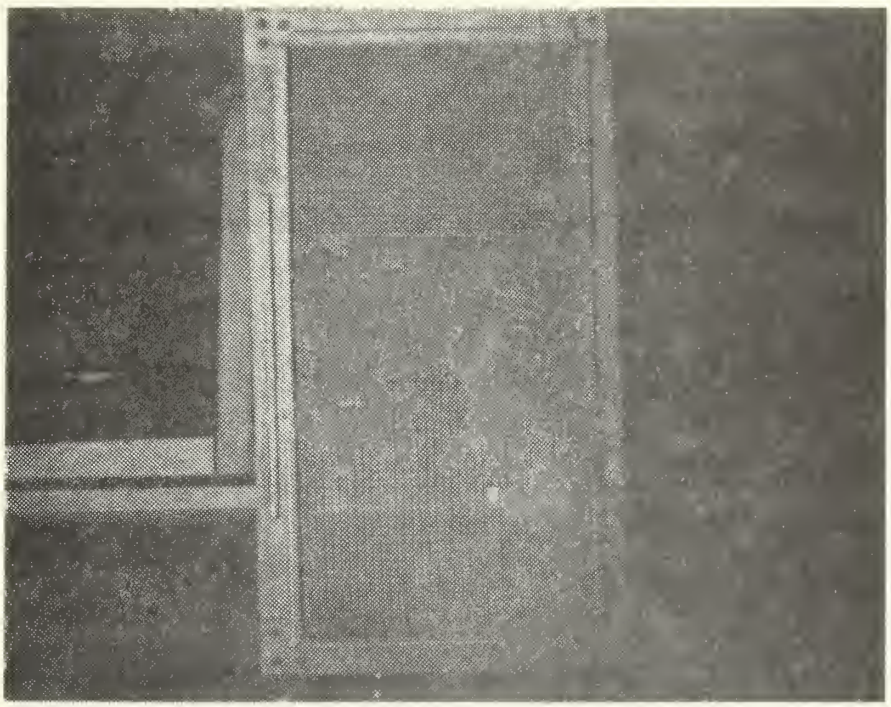

FIGURE 3. Plywood Form With Wire Mesh

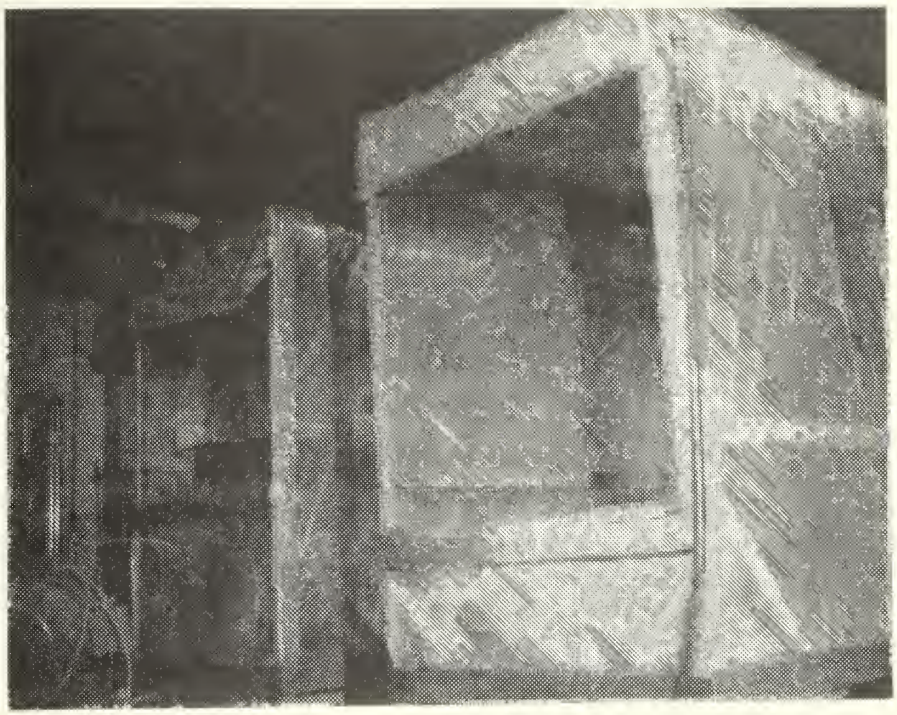

FIGURE 4. Specimen Curing Tents

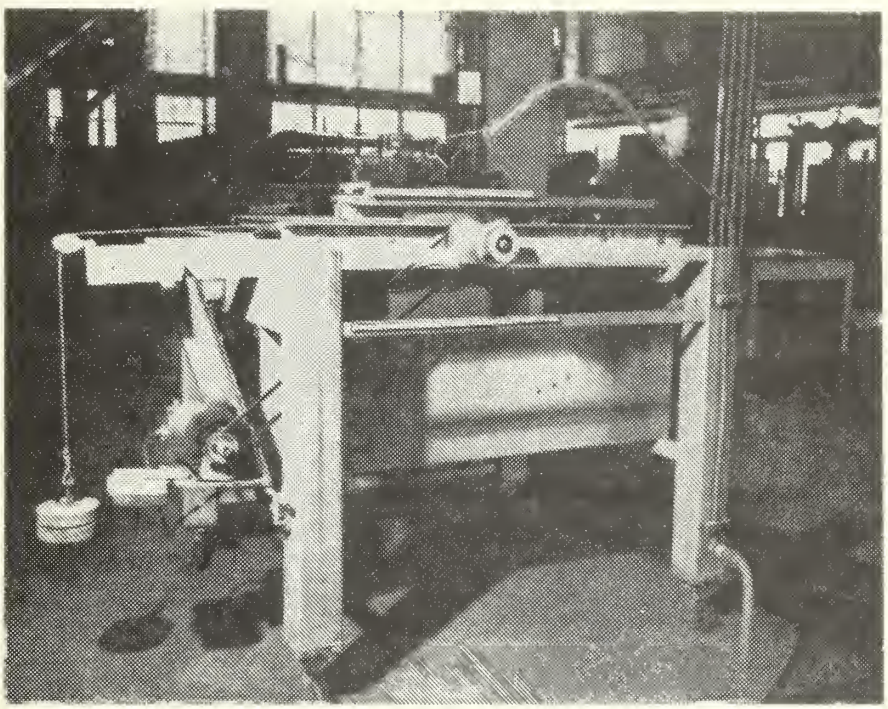

FIGURE 5. Saw for Cutting Specimens from Panels

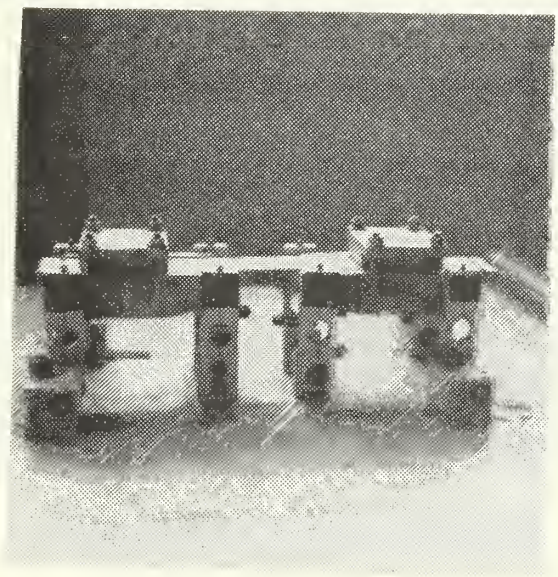

FIGURE 6. Fatigue Testing Jig

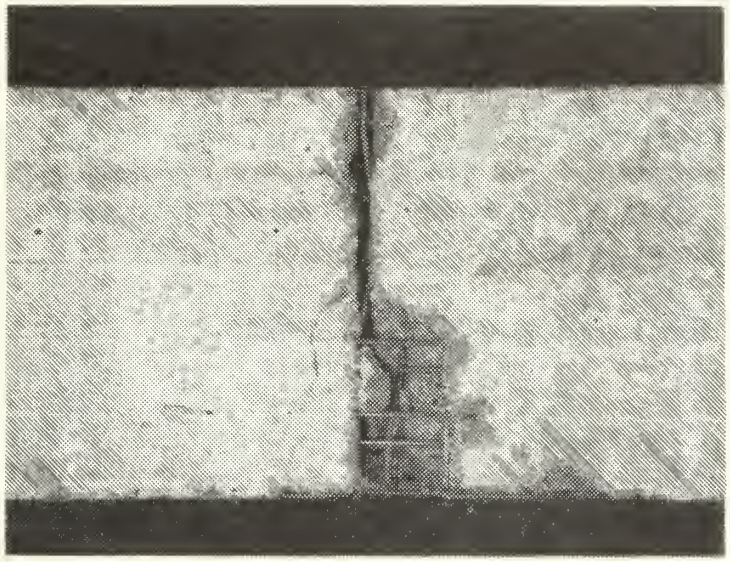

FIGURE 7. Close-Up of Fatigue Failure at Maximum Deflection of Three-Quarters of an Inch

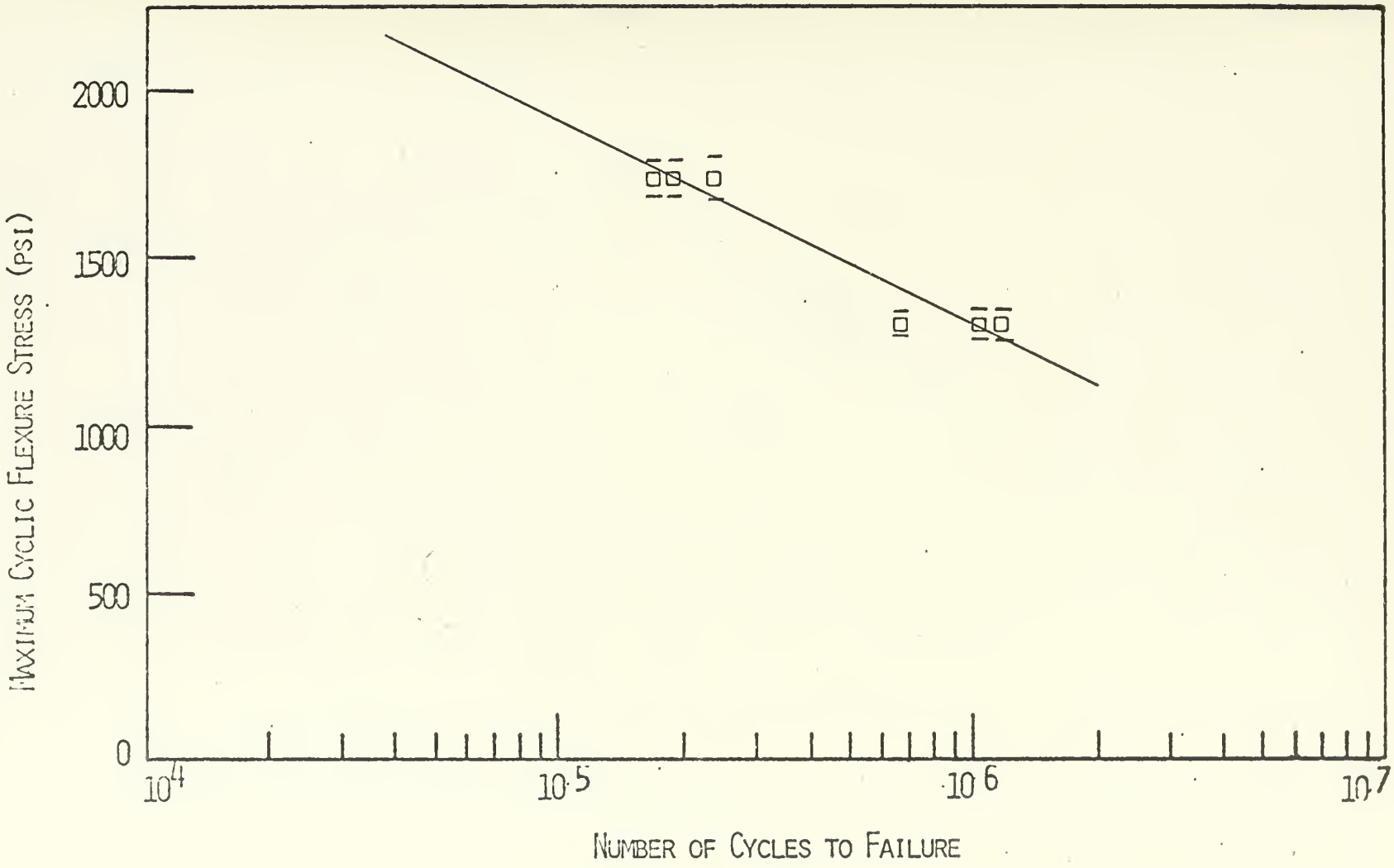

FIGURE 8. S_f-N Plot for Panel QUL7S3, All Layers With Stronger Wires Parallel to Specimen Axis

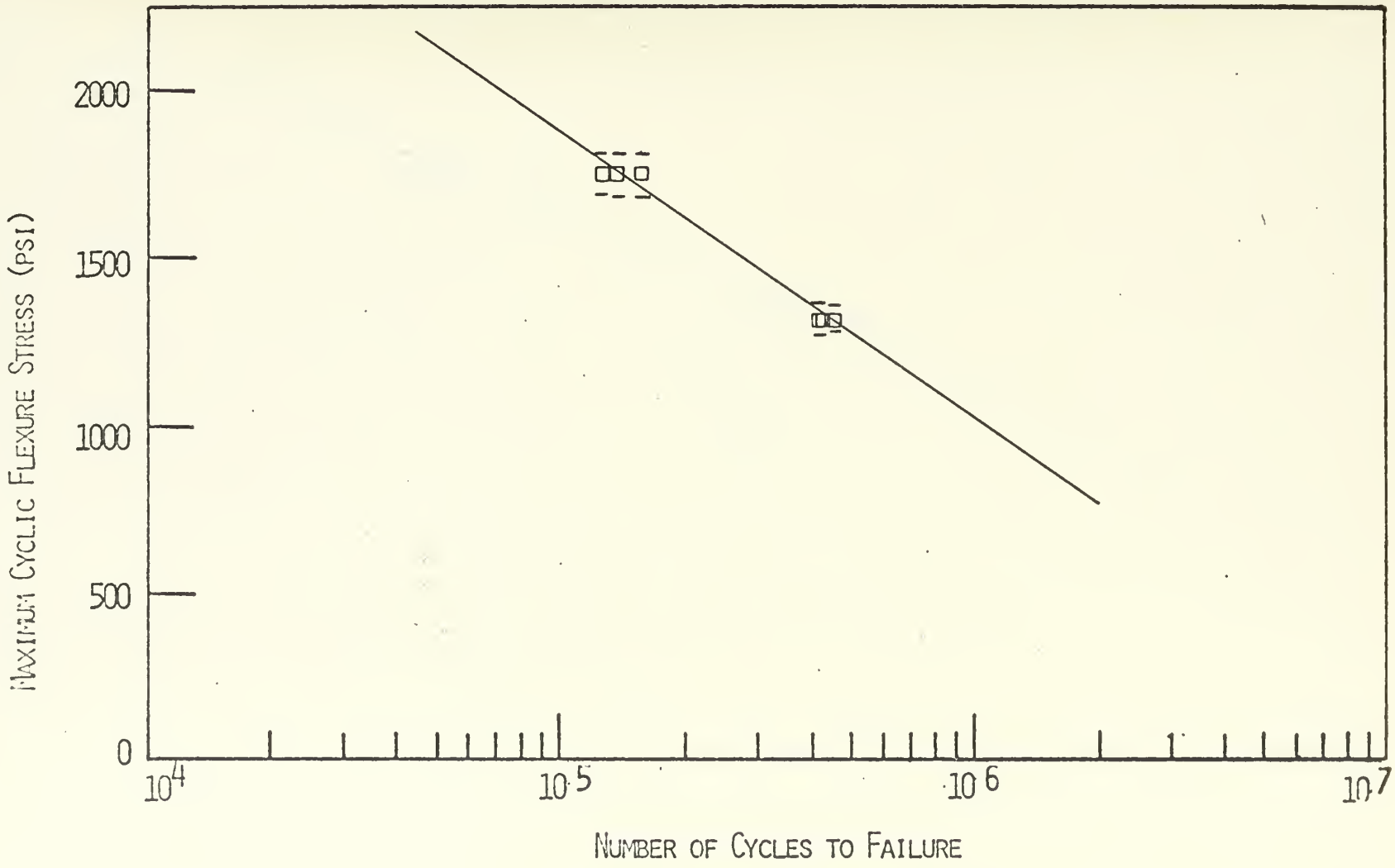

FIGURE 9. S_f-N Plot for Panel QUA7S1, Both Outer, and Each Alternate Layer With Stronger Wires Parallel to Specimen Axis

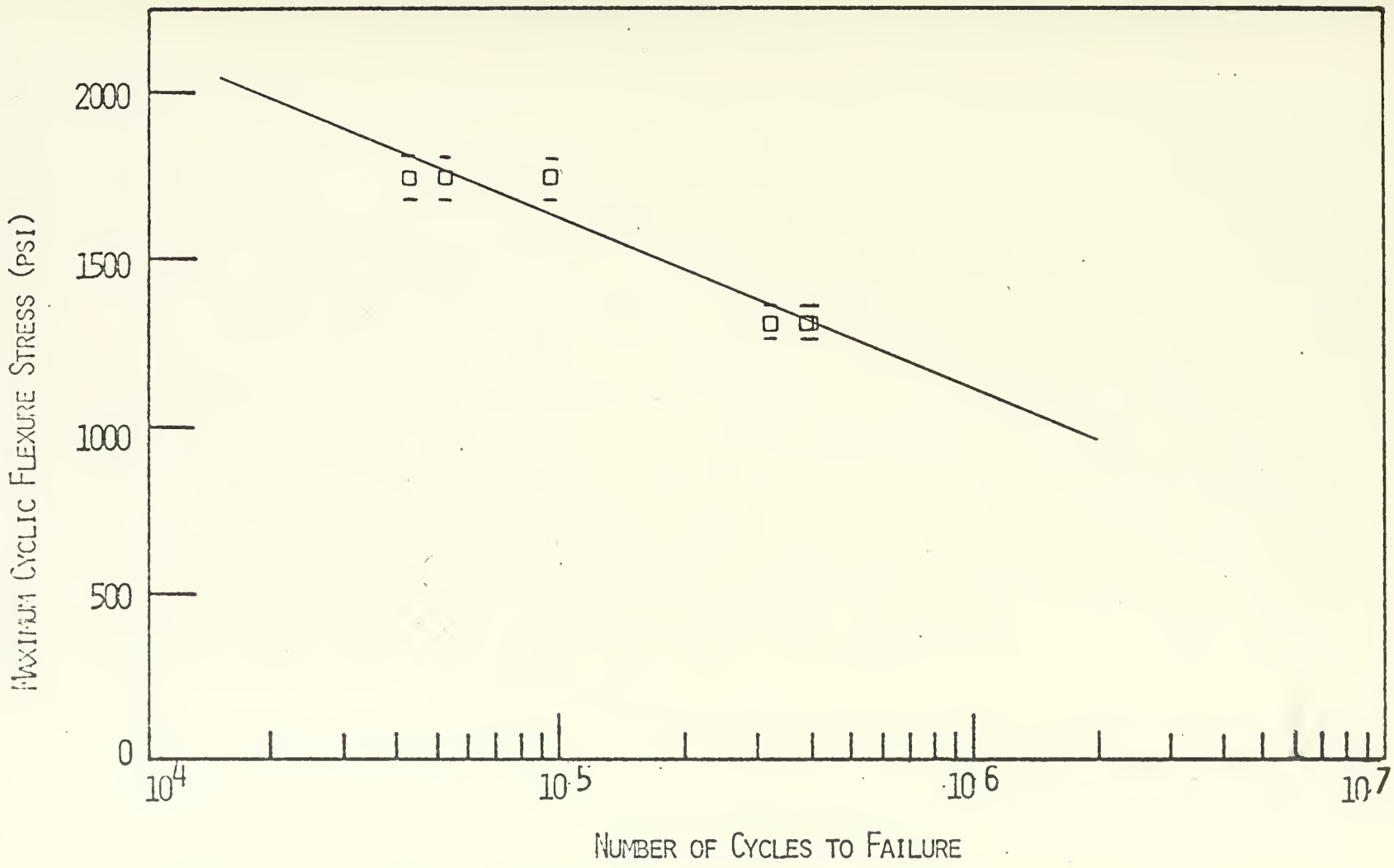

FIGURE 10. S_f-N Plot for Panel QUB7S1, Both Outer, and Each Alternate Layer With Weaker Wires Parallel to Specimen Axis

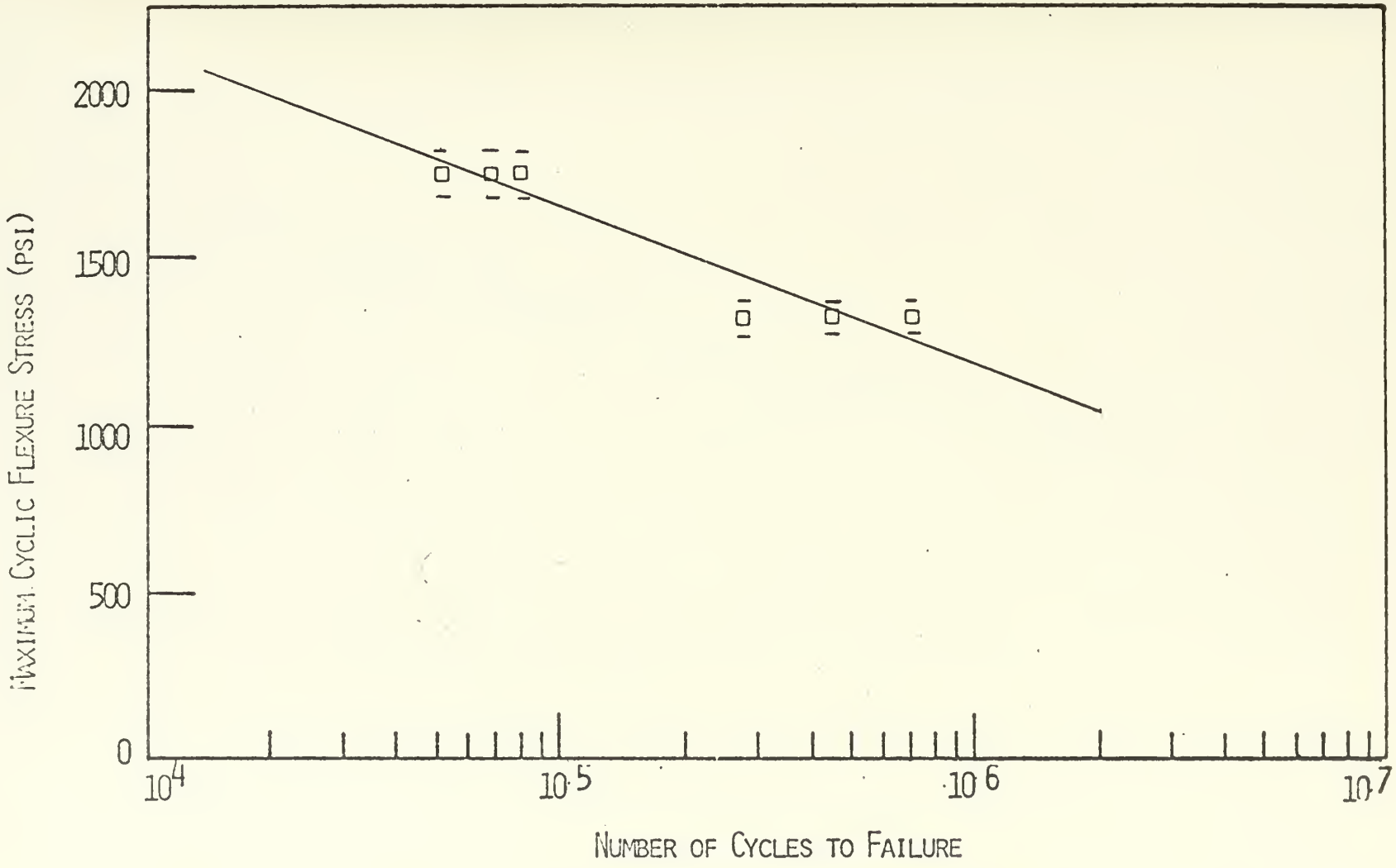

FIGURE 11. S_f-N Plot for Panel QUT7S2, All Layers With Weaker Wires Parallel to Specimen Axis, One Side With Outermost Wires Perpendicular to Axis

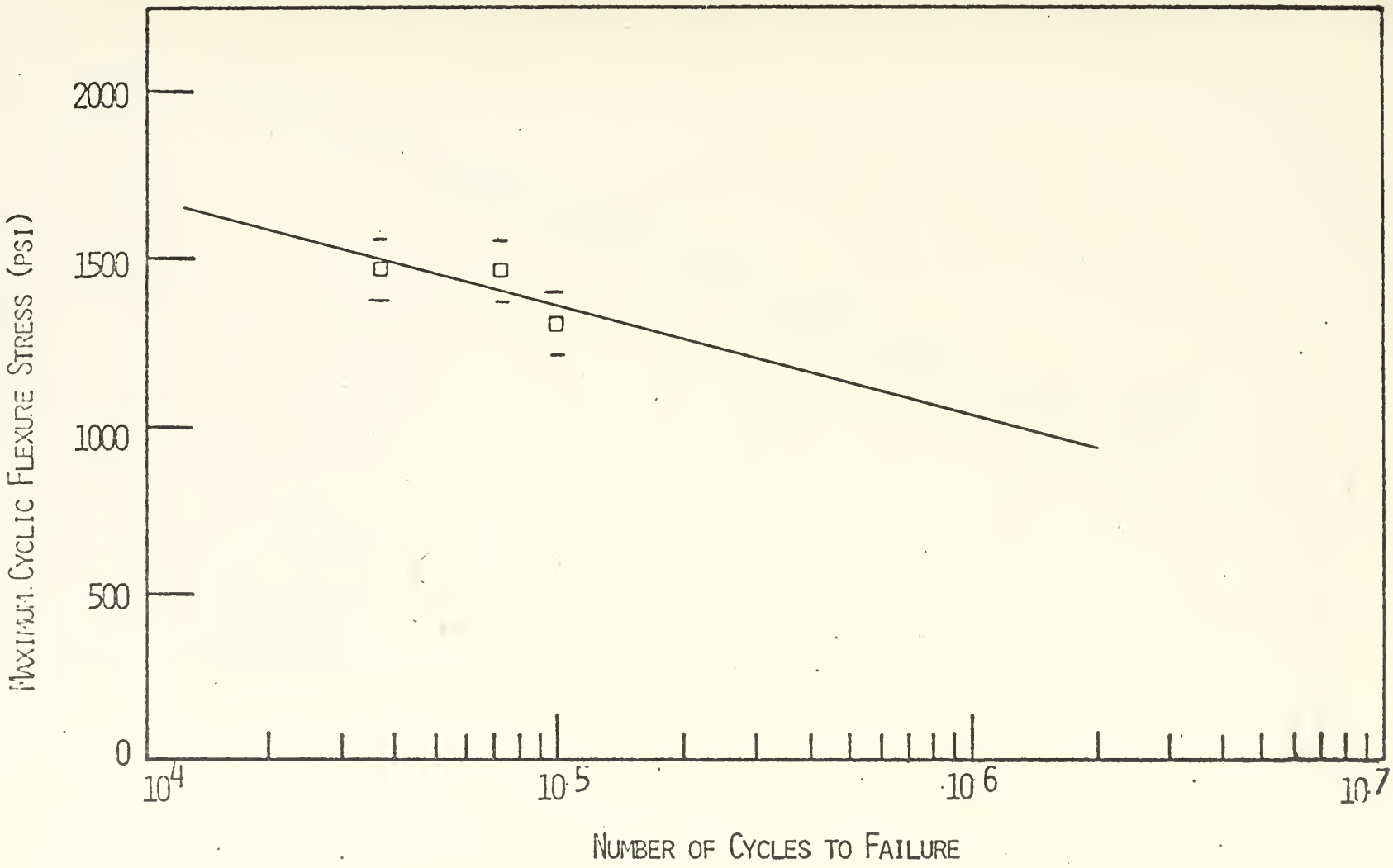

FIGURE 12. S_f-N Plot for Panel QUA7S1, Cut With Weaker Wires Parallel to Specimen Axis, Outermost Wires Perpendicular to Axis

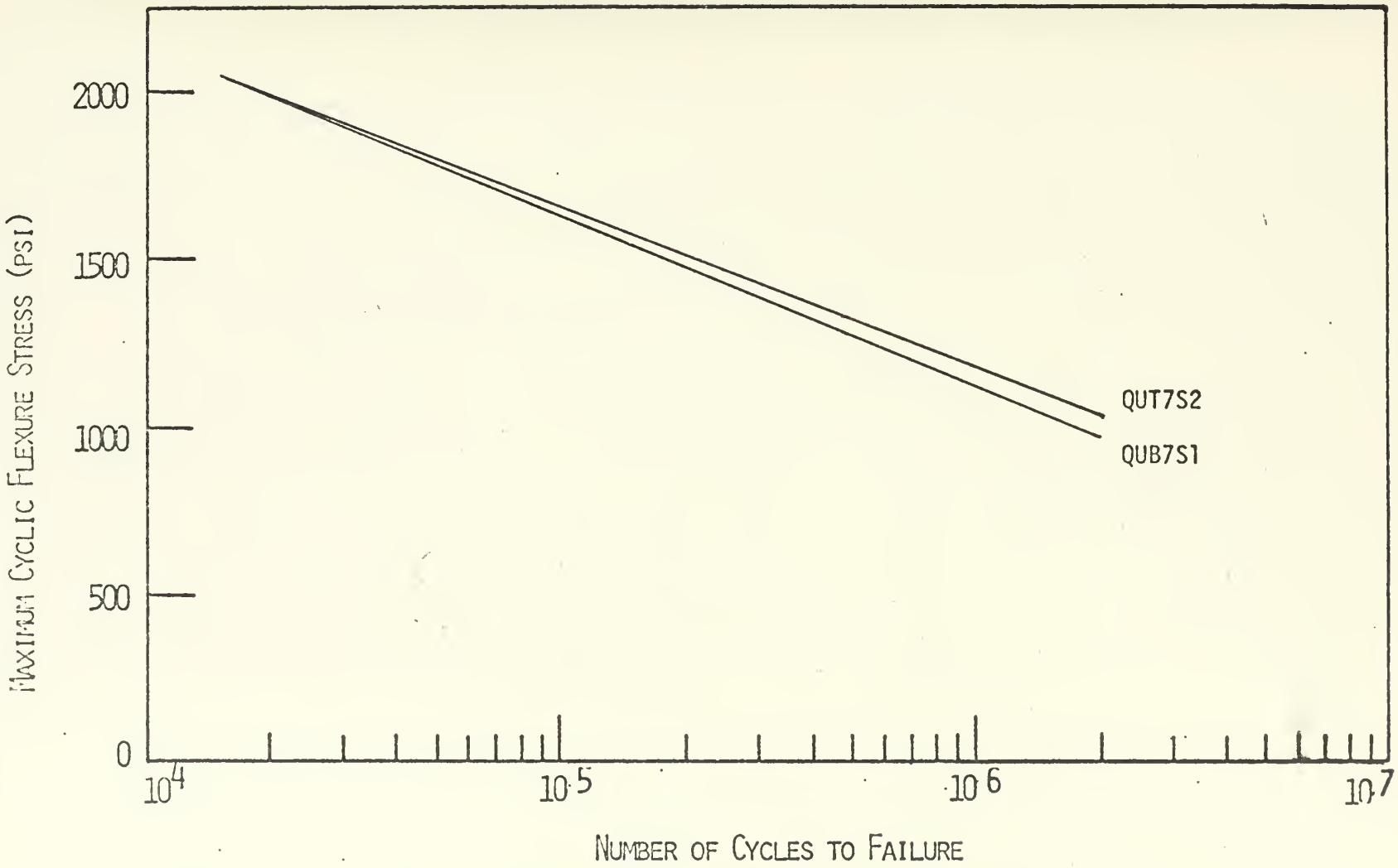

FIGURE 13. S_f-N Plot Comparing Results of Panels QUT7S2 and QUB7S1

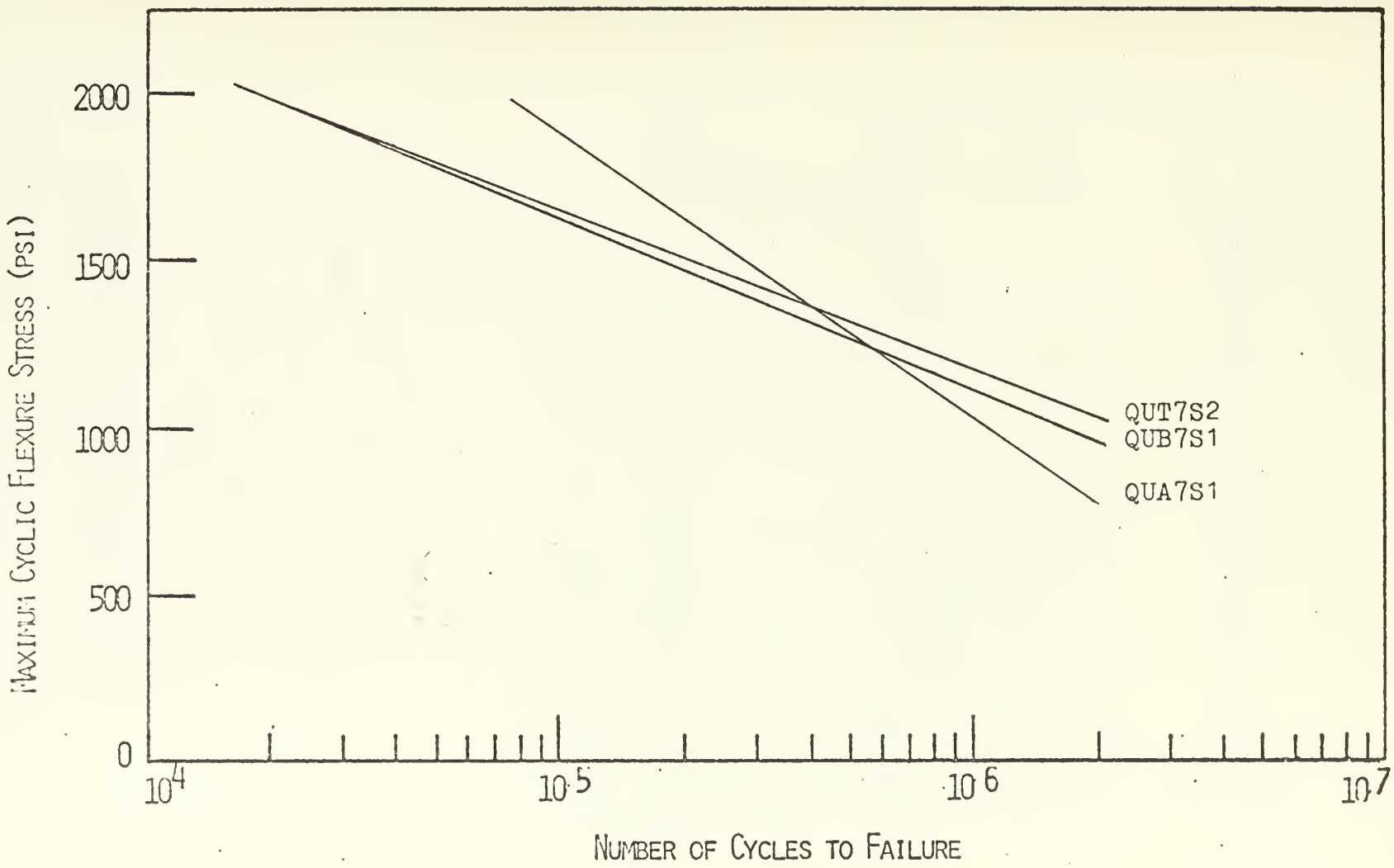

FIGURE 14. S_f-N Plot Comparing Results for Panels QUT7S2, QUB7S1, and QUA7S1 With Stronger Wires Parallel to Specimen Axis

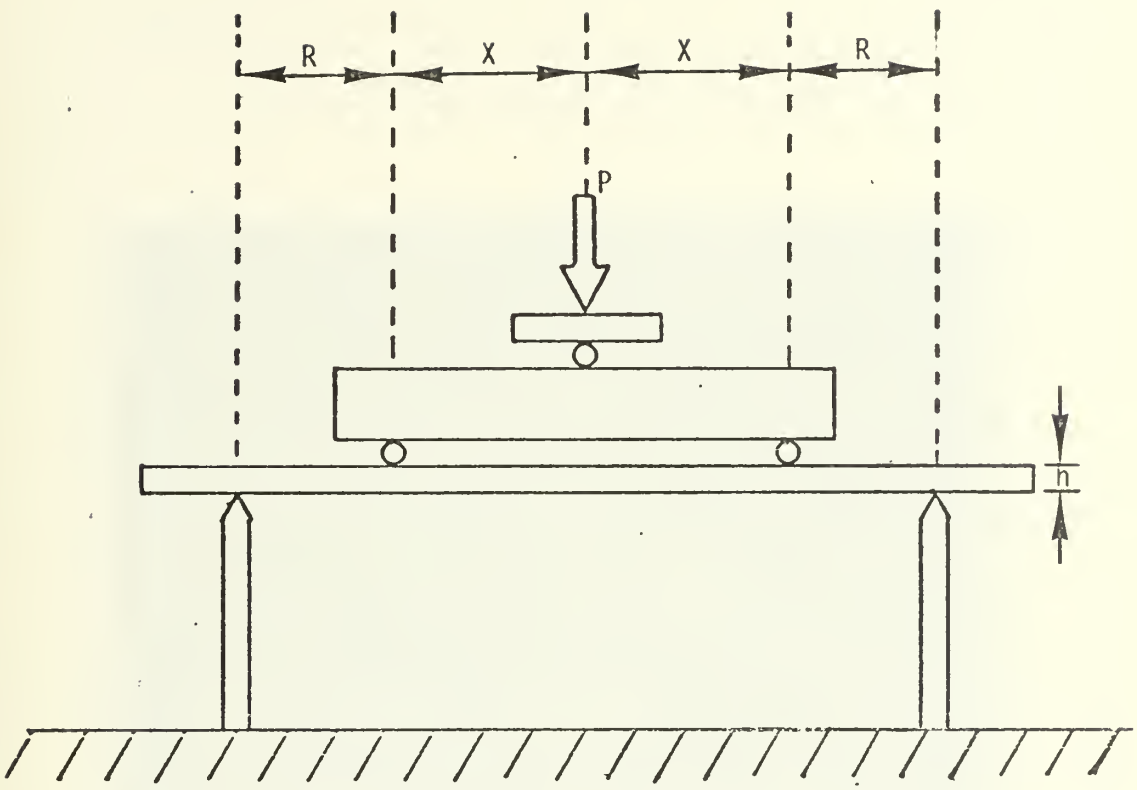

R = 3 inches

X = 4 inches

h = specimen thickness (inches)

P = applied load (lbf)

FIGURE 15. Sketch of Monotonic Bending Scheme

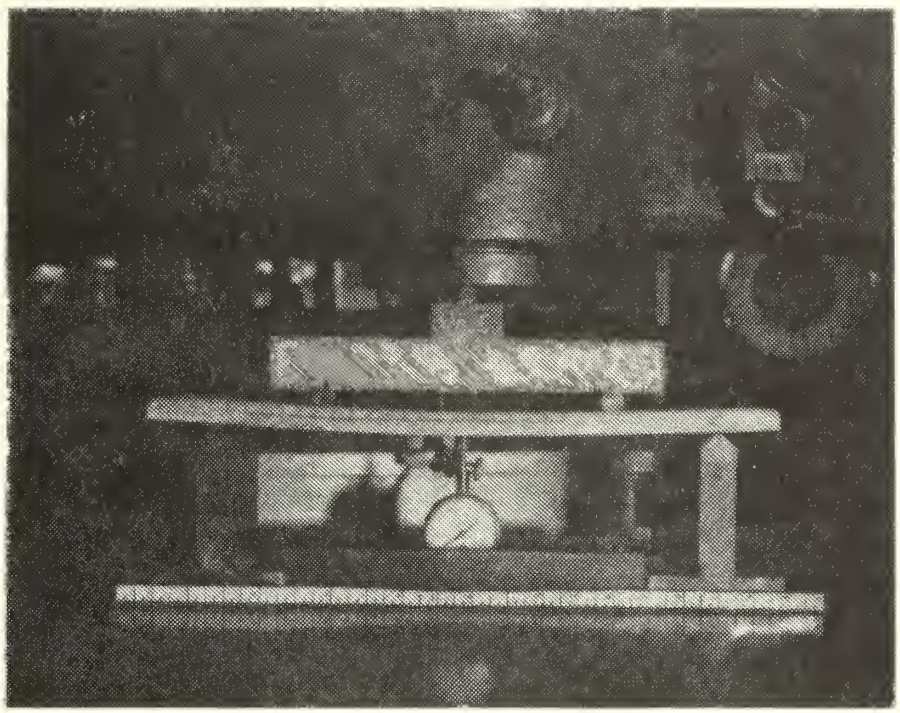

FIGURE 16. Monotonic Bending Jig

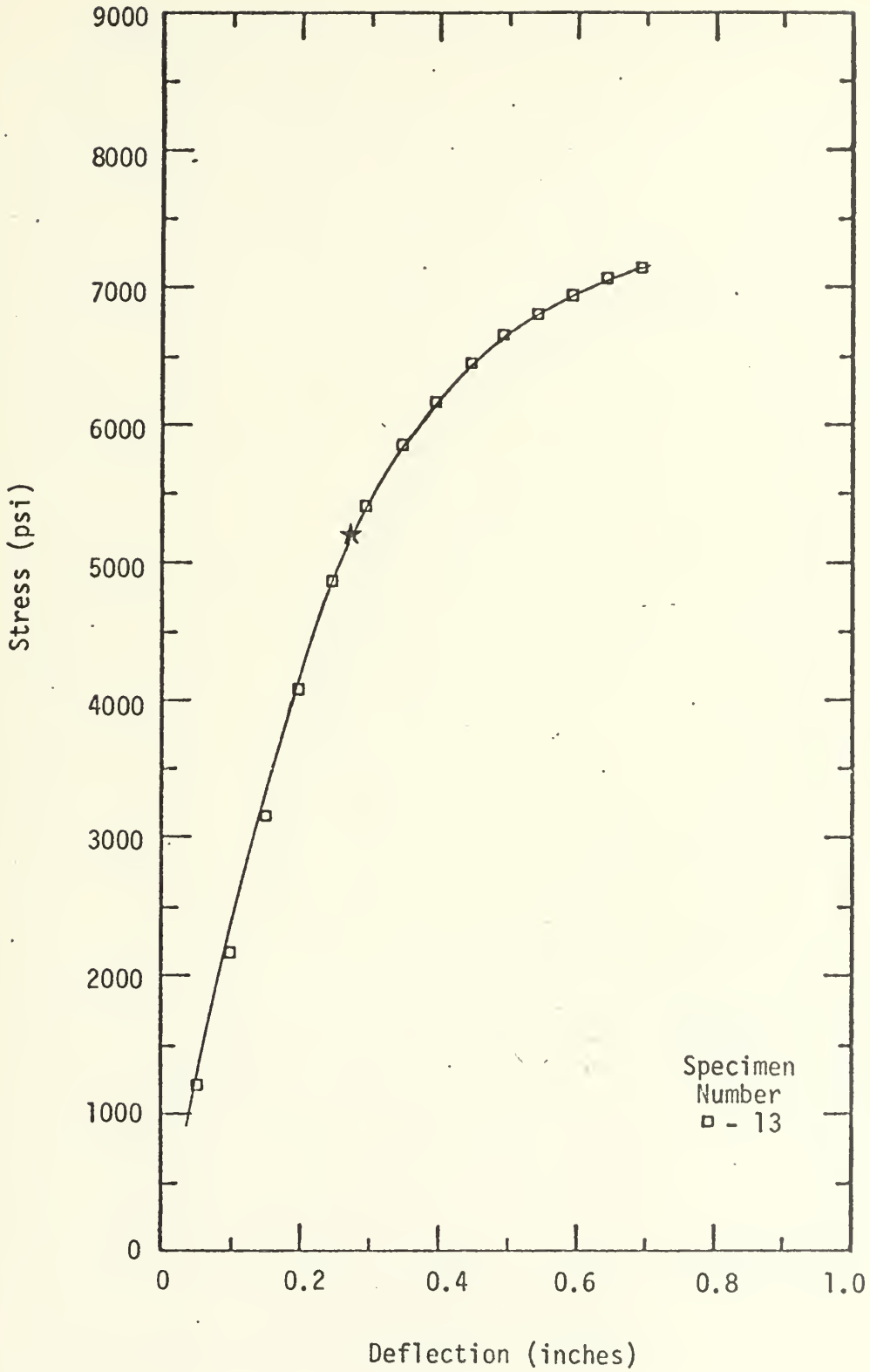

FIGURE 17. Monotonic Bending Stress vs. Deflection Plot for Panel QUA7S1

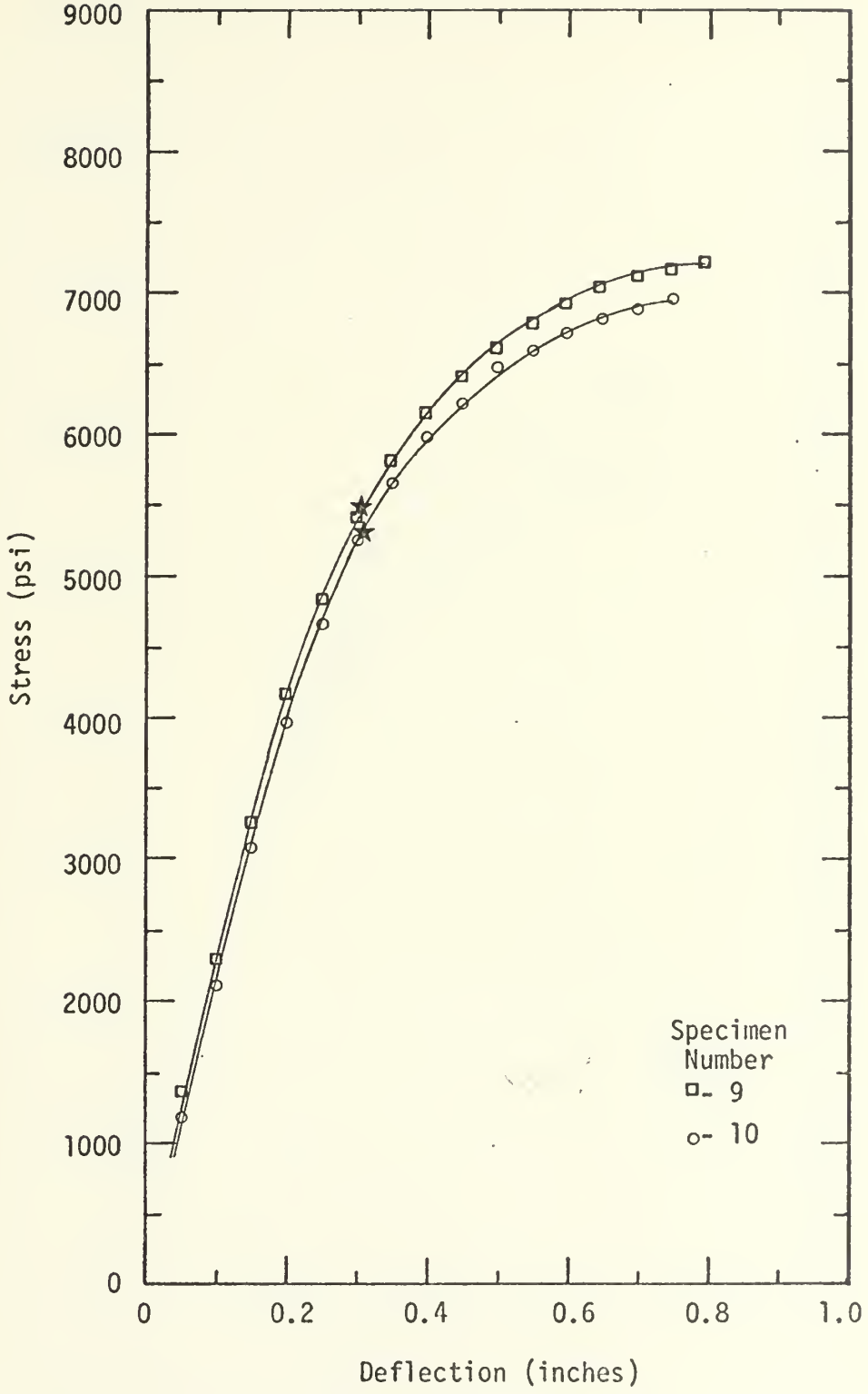

FIGURE 18. Monotonic Bending Stress vs. Deflection Plot for Panel QUT7S2

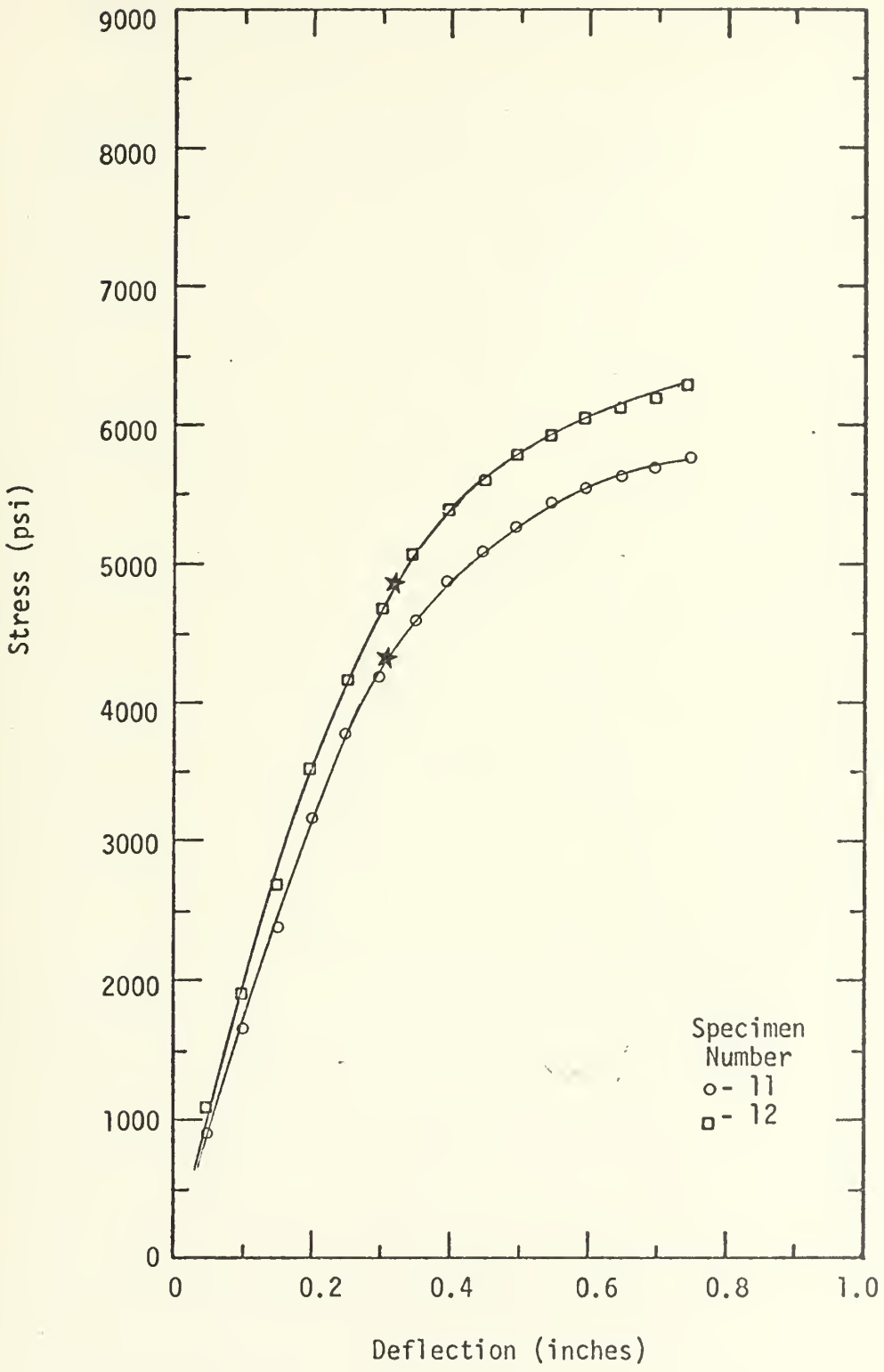

FIGURE 19. Monotonic Bending Stress vs. Deflection Plot for Panel QUT7S2

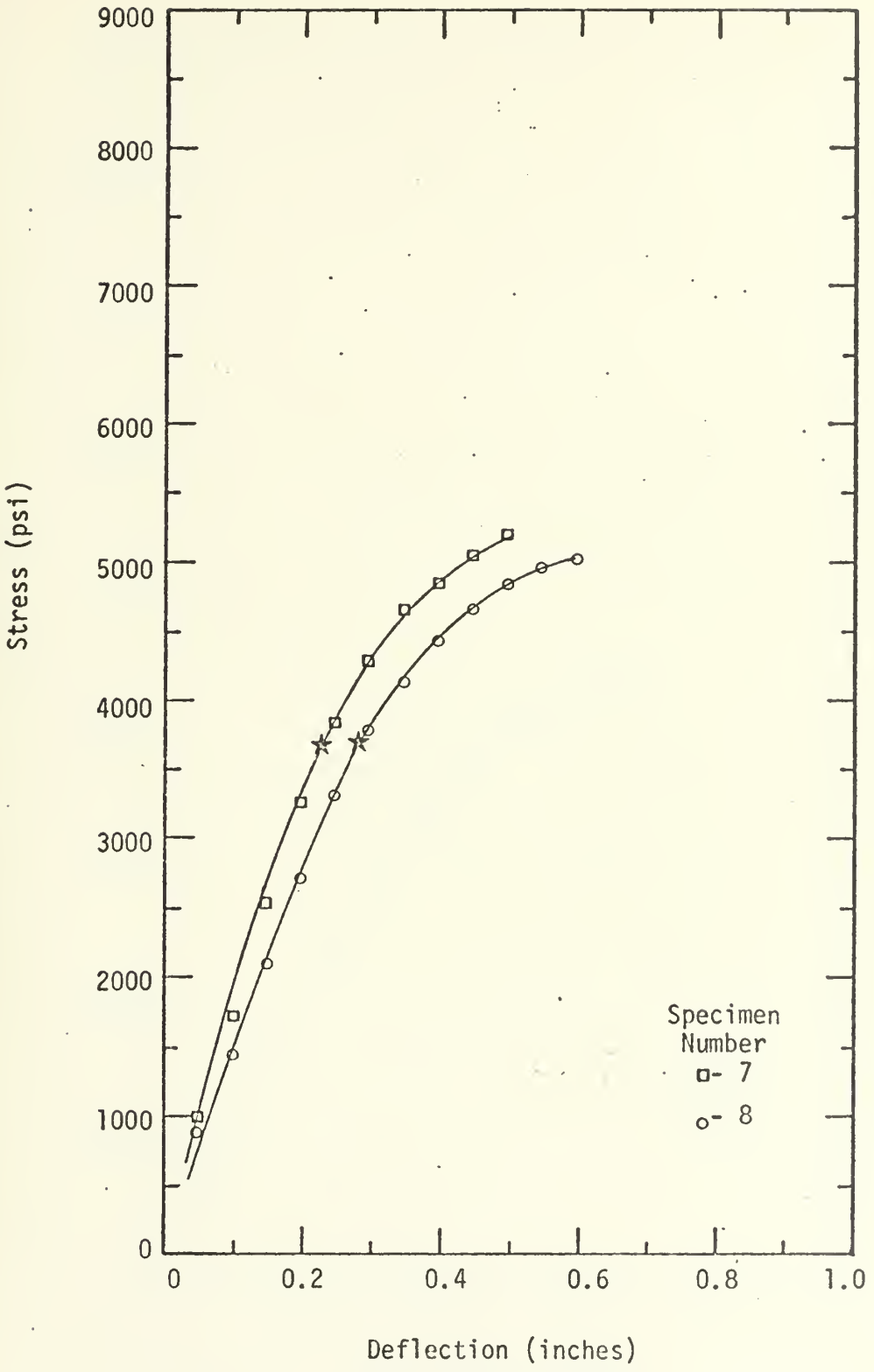

FIGURE 20. Monotonic Bending Stress vs. Deflection Plot for Panel QUL7S3

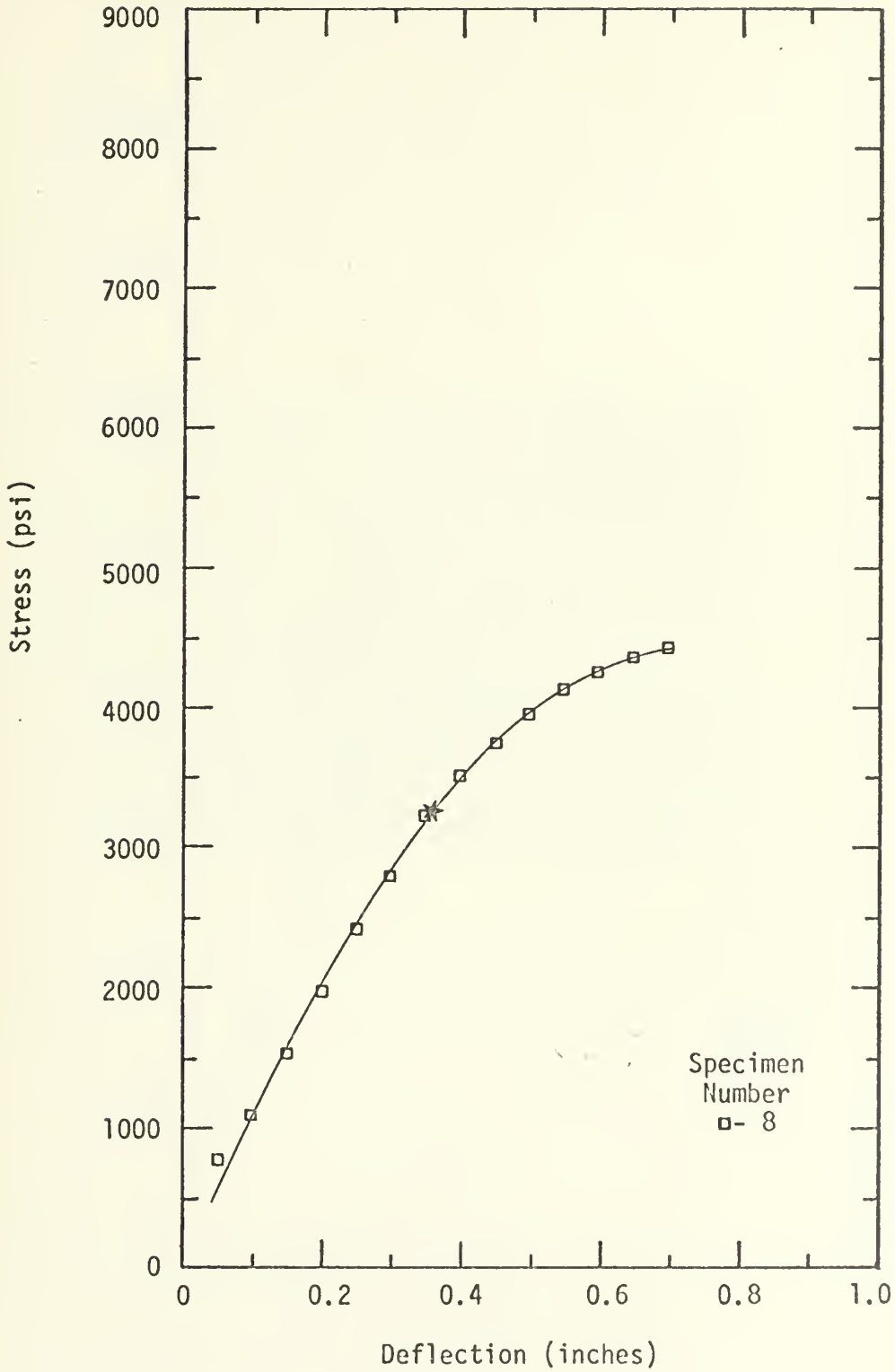

FIGURE 21. Monotonic Bending Stress vs. Deflection Plot for Panel QUA7S1

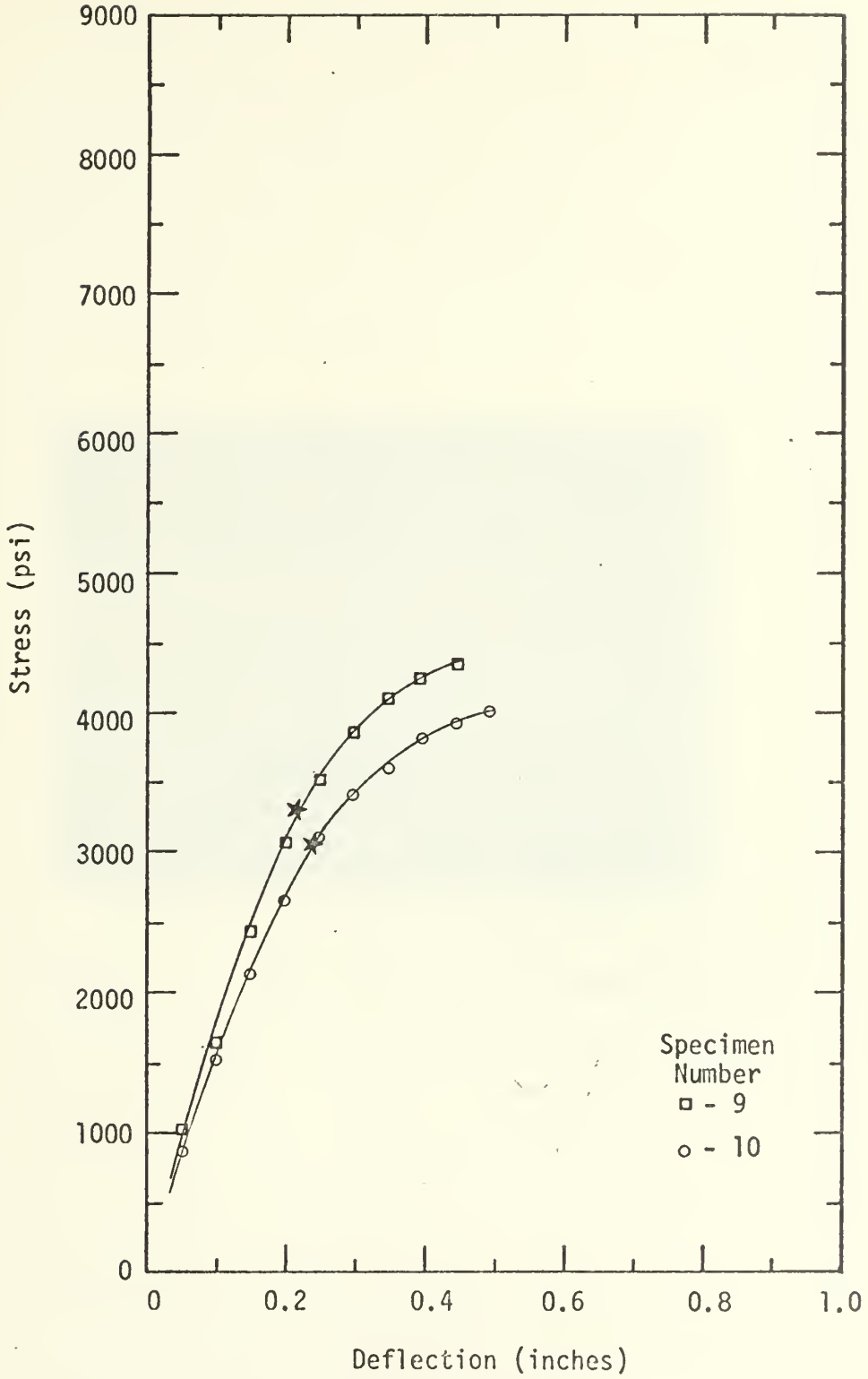

FIGURE 22. Monotonic Bending Stress vs. Deflection Plot for Panel QUB7S1

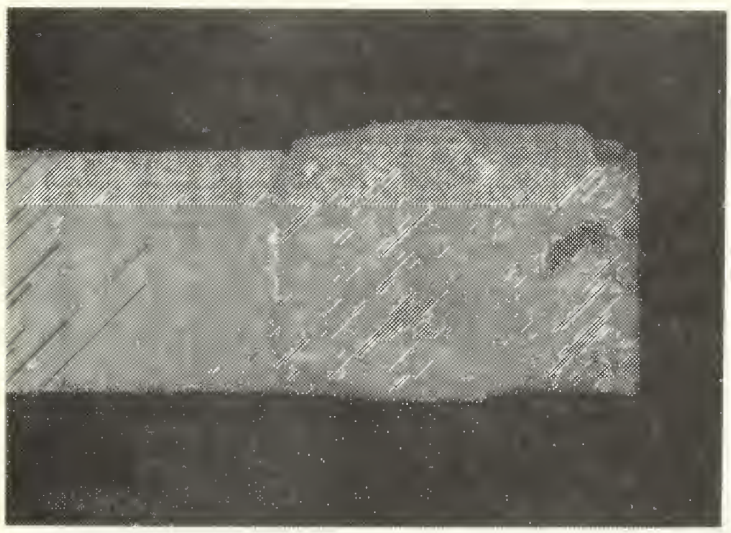

FIGURE 23. Epoxy Coating on Tensile Specimen

FIGURE 24. Tensile Failure Along Cleavage Plane Caused By Alignment of Mesh Layers

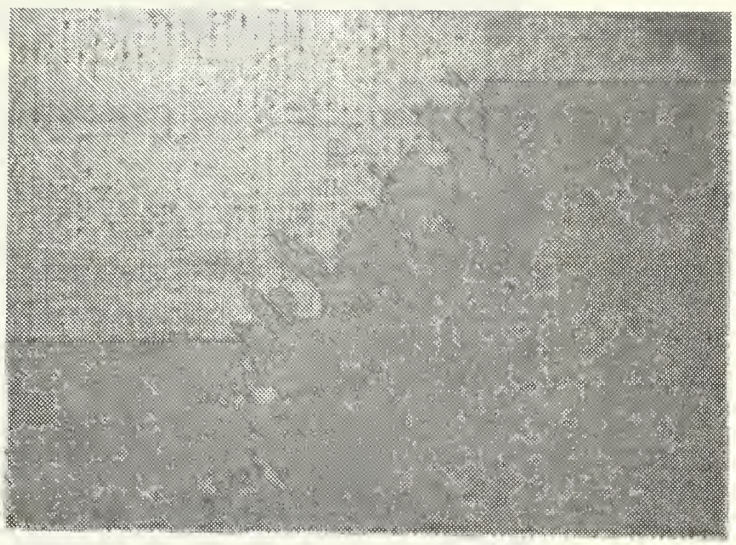

FIGURE 25. Poorly Impregnated Panel Before Cutting

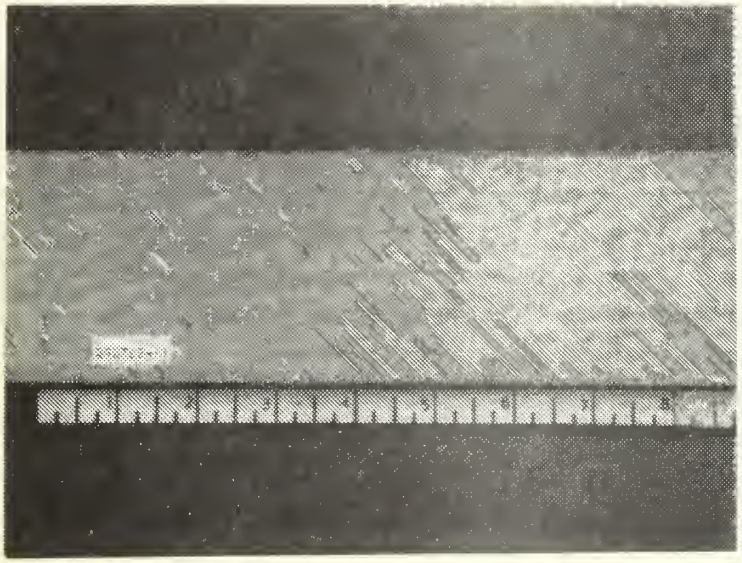

(a) Before Cyclic Loading

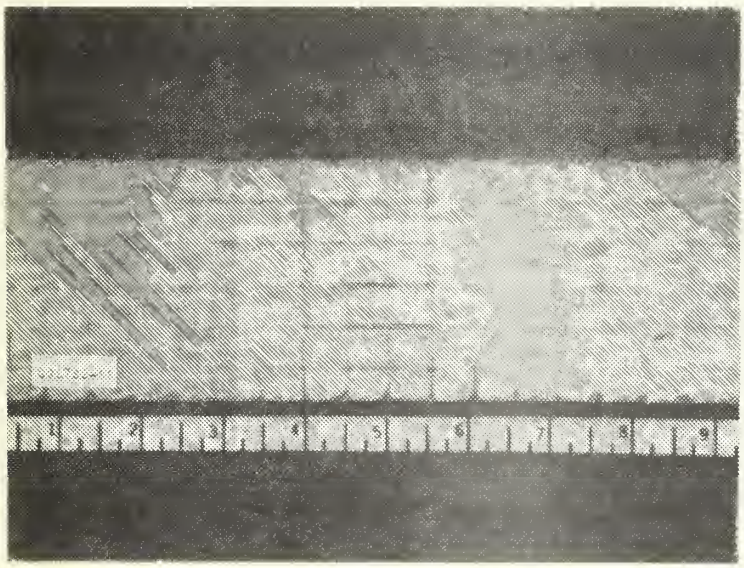

(b) After Fatigue Failure

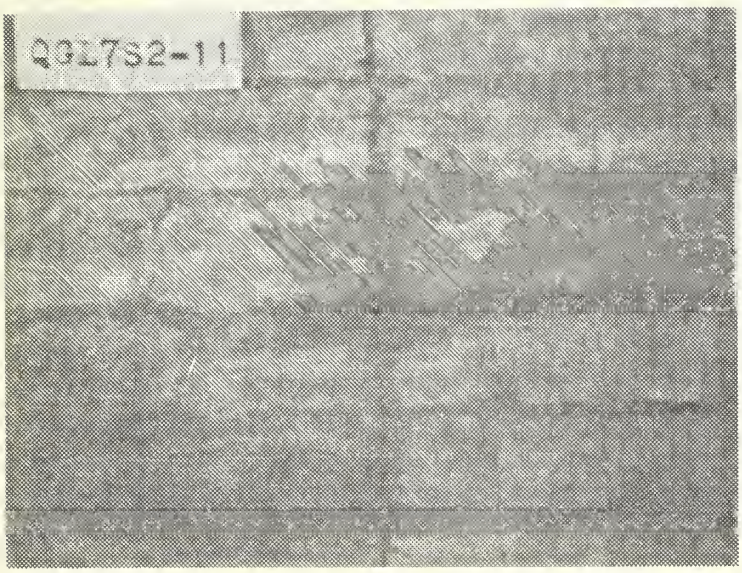

(c) Close-Up of (b)

FIGURE 26. Views of Specimen QGL7S2-11

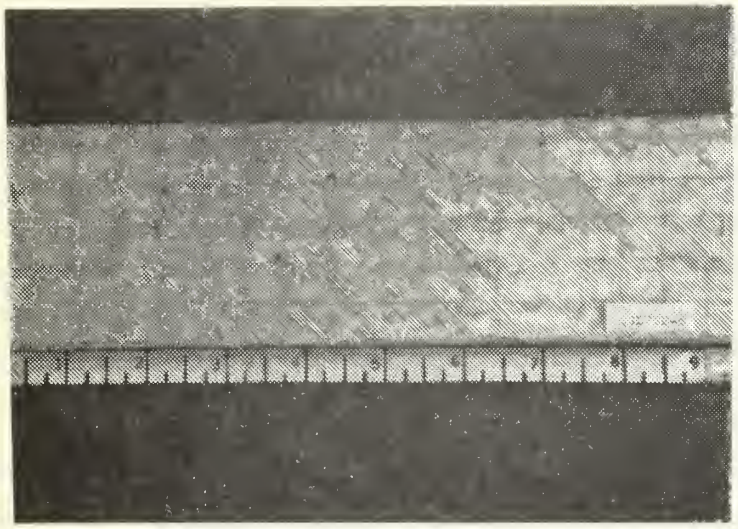

(a) Before Cyclic Loading

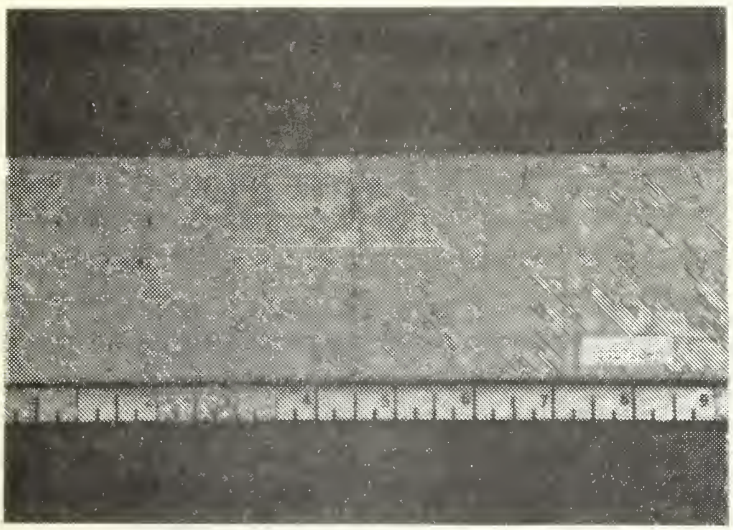

(b) After Fatigue Failure

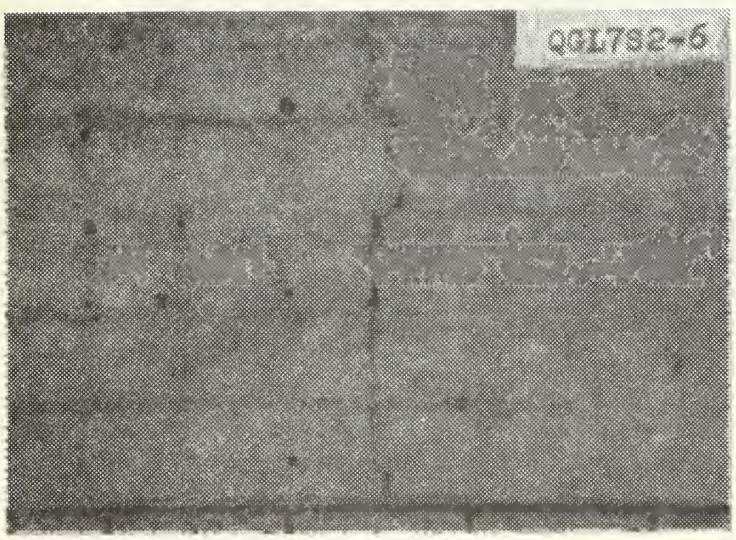

(c) Close-Up of (b)

FIGURE 27. Views of Specimen QGL7S2-6

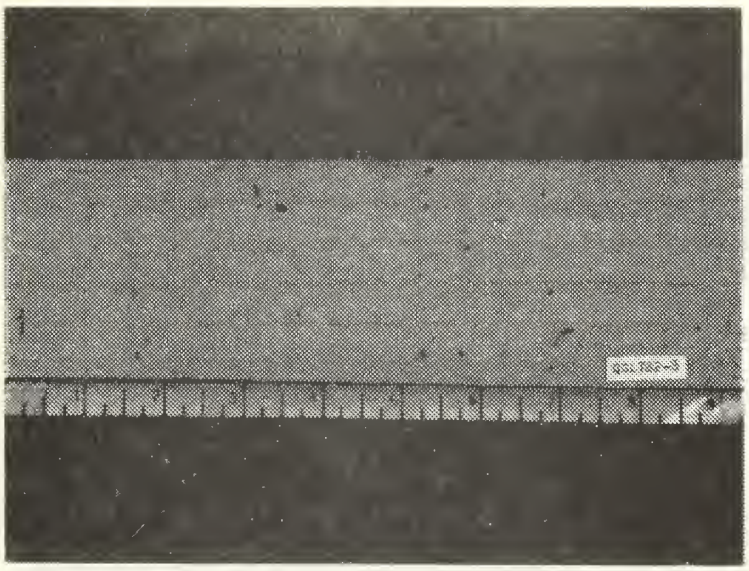

(a) Before Cyclic Loading

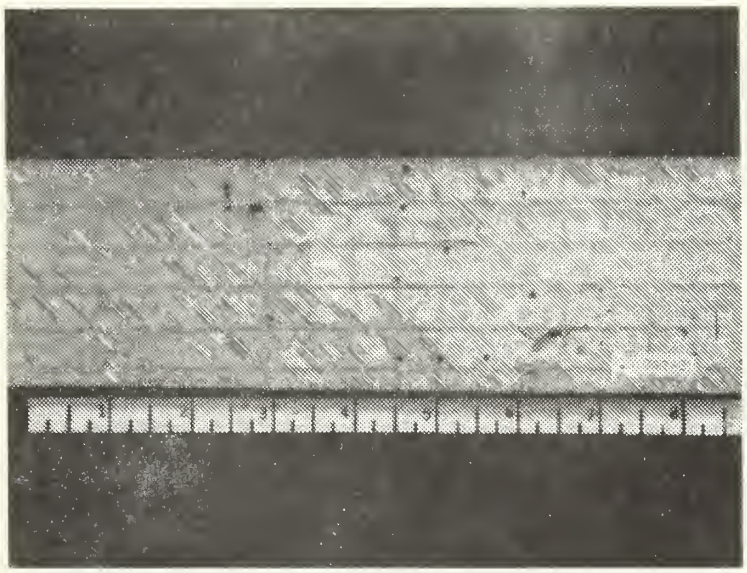

(b) After Fatigue Failure

FIGURE 28. Views of Specimen QGL7S2-8

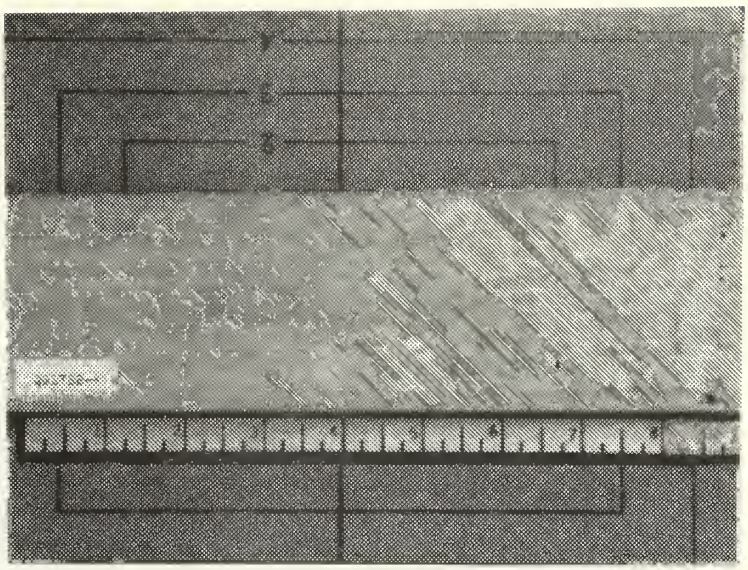

(a) Before Cyclic Loading

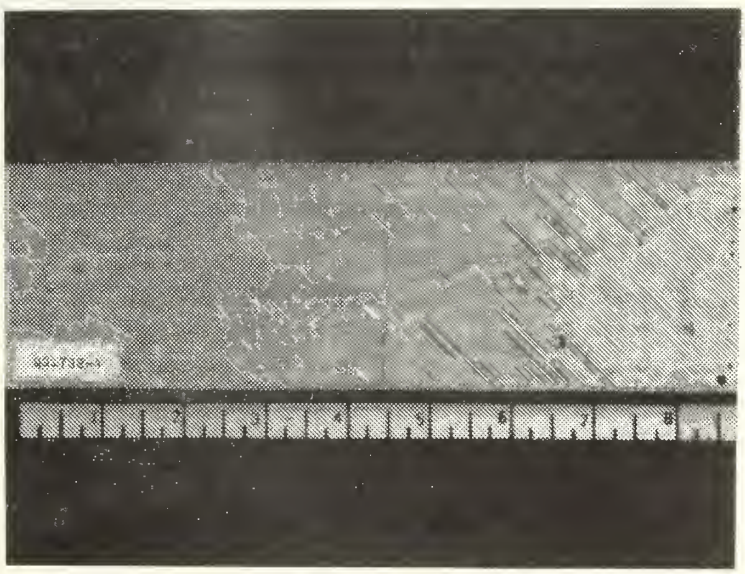

(b) After Fatigue Failure

FIGURE 29. Views of Specimen QGL7S2-4

FIGURE 30. Edge View of Specimen QGL7S2-4 Showing Fatigue Crack

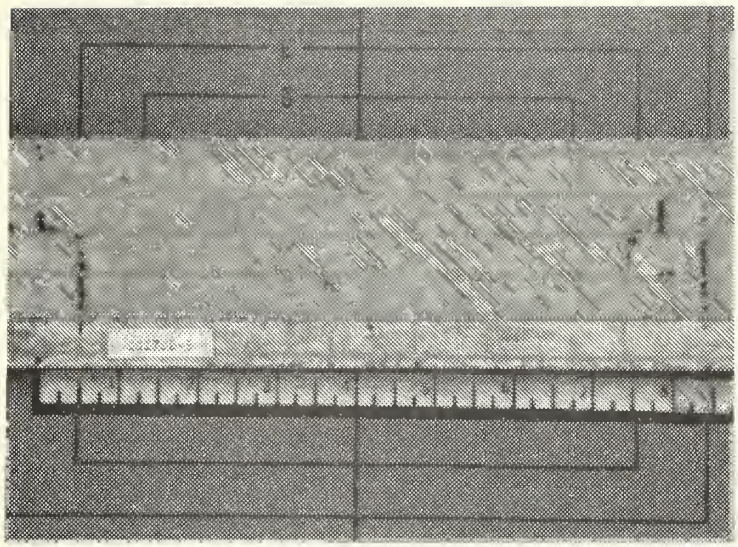

(a) Before Cyclic Loading

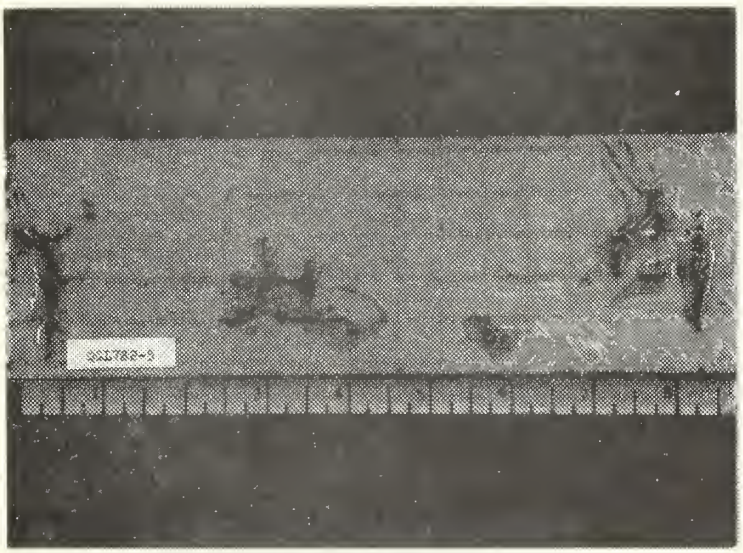

(b) After Fatigue Failure

FIGURE 31. Views of Specimen QGL7S2-5

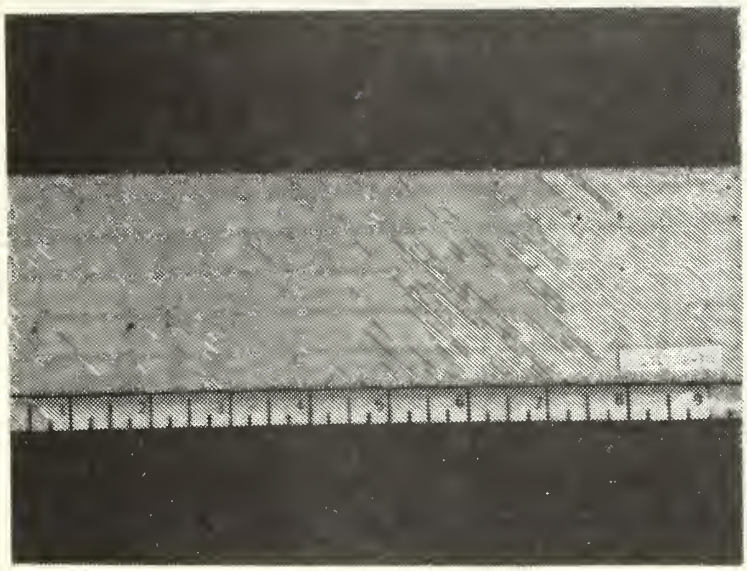

(a) Before Cyclic Loading

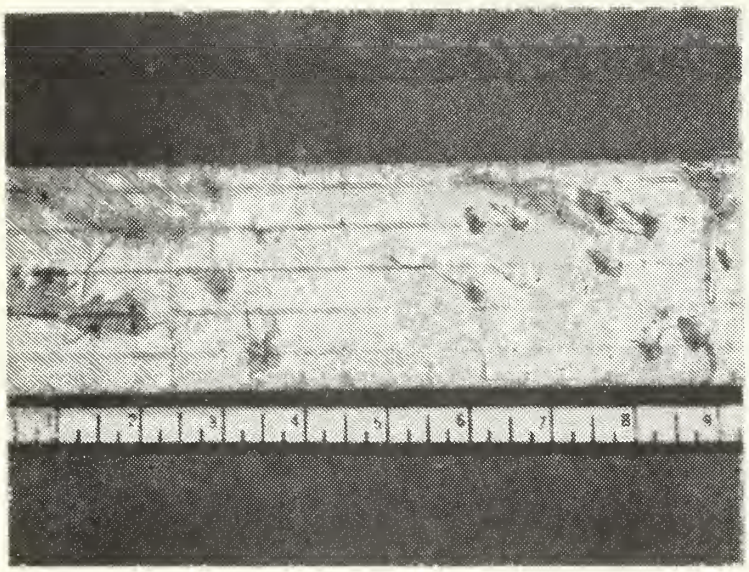

(b) After Fatigue Failure

FIGURE 32. Views of Specimen QGL7S2-10

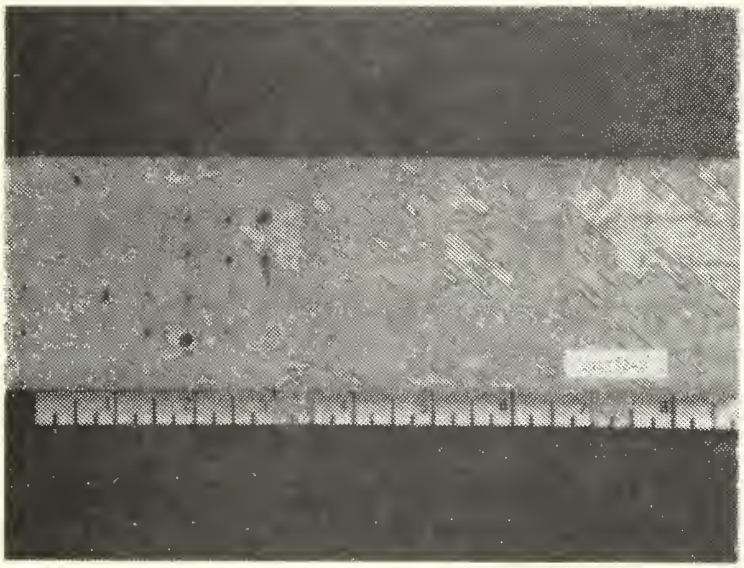

(a) Before Cyclic Loading

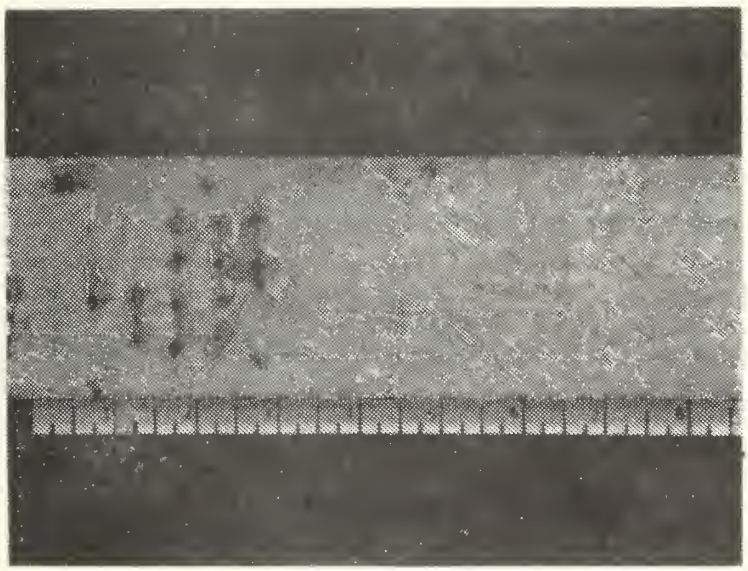

(b) After Fatigue Failure

FIGURE 33. Views of Specimen QGL7S2-2

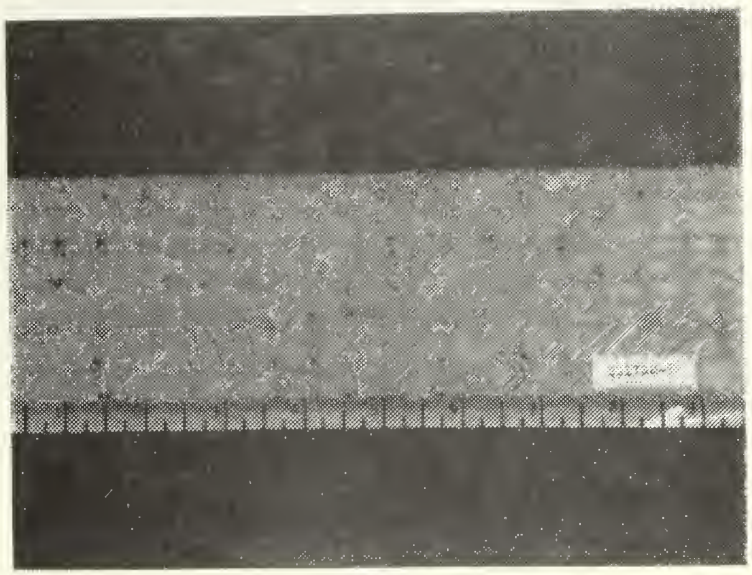

(a) Before Cyclic Loading

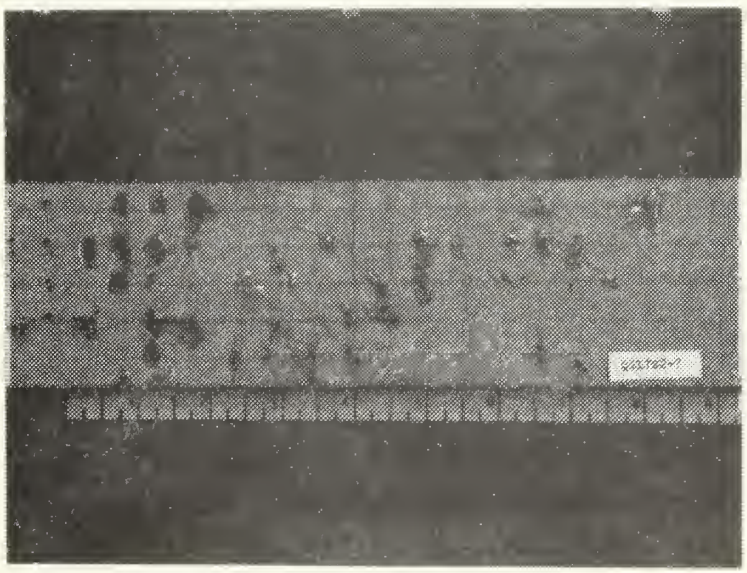

(b) After Fatigue Failure

FIGURE 34. Views of Specimen QGL7S2-7

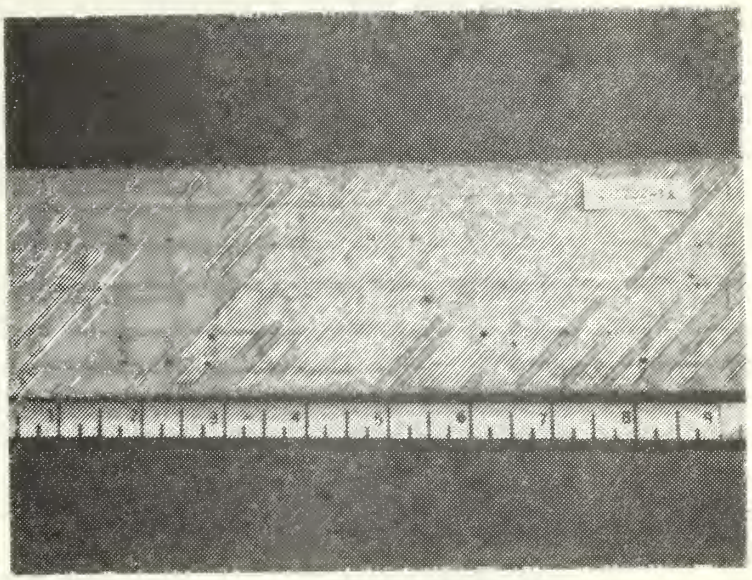

(a) Before Monotonic Bending

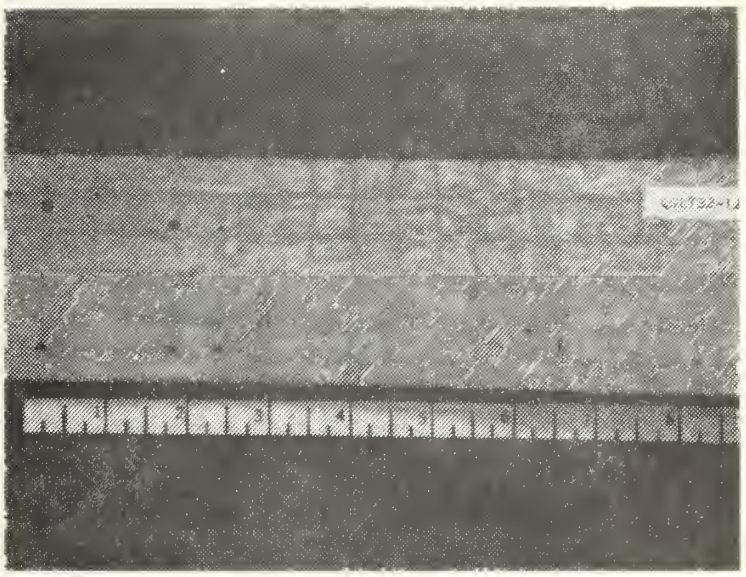

(b) After Monotonic Bending Failure

FIGURE 35. Views of Specimen OGL7S2-1A

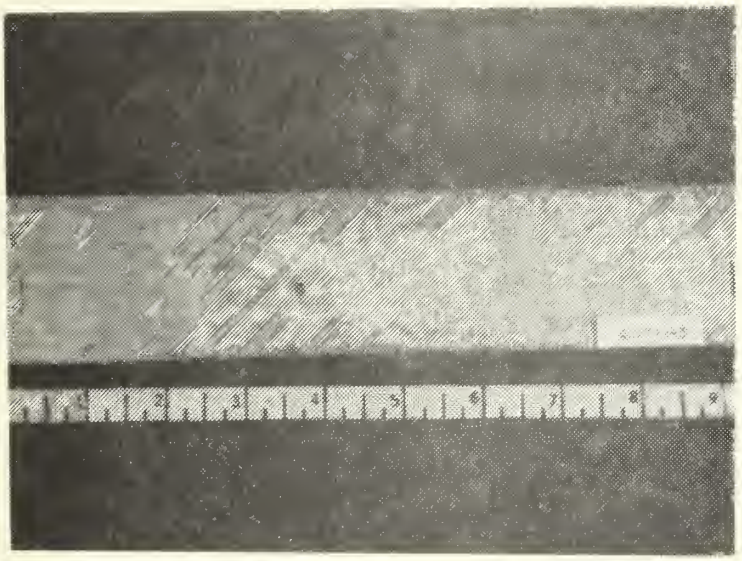

(a) Before Monotonic Bending

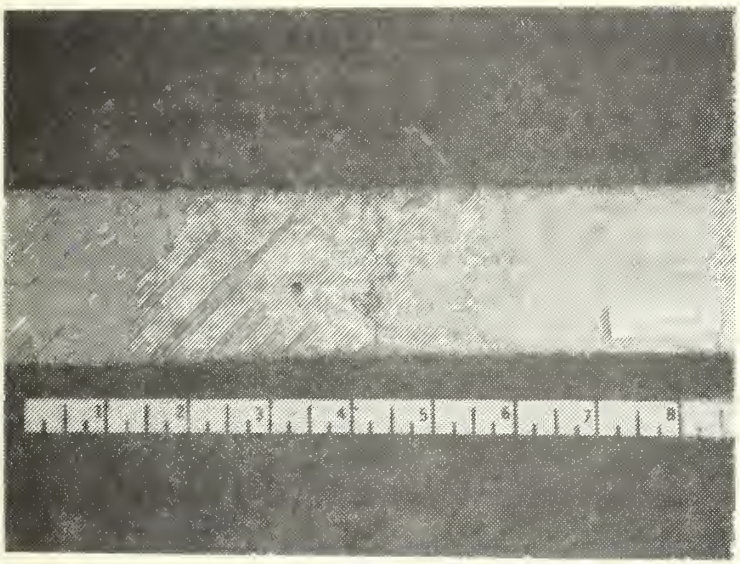

(b) Inside of Curve After Monotonic Failure

(c) Edge View after Monotonic Failure

FIGURE 36. Views of Specimen QGL7S2-3

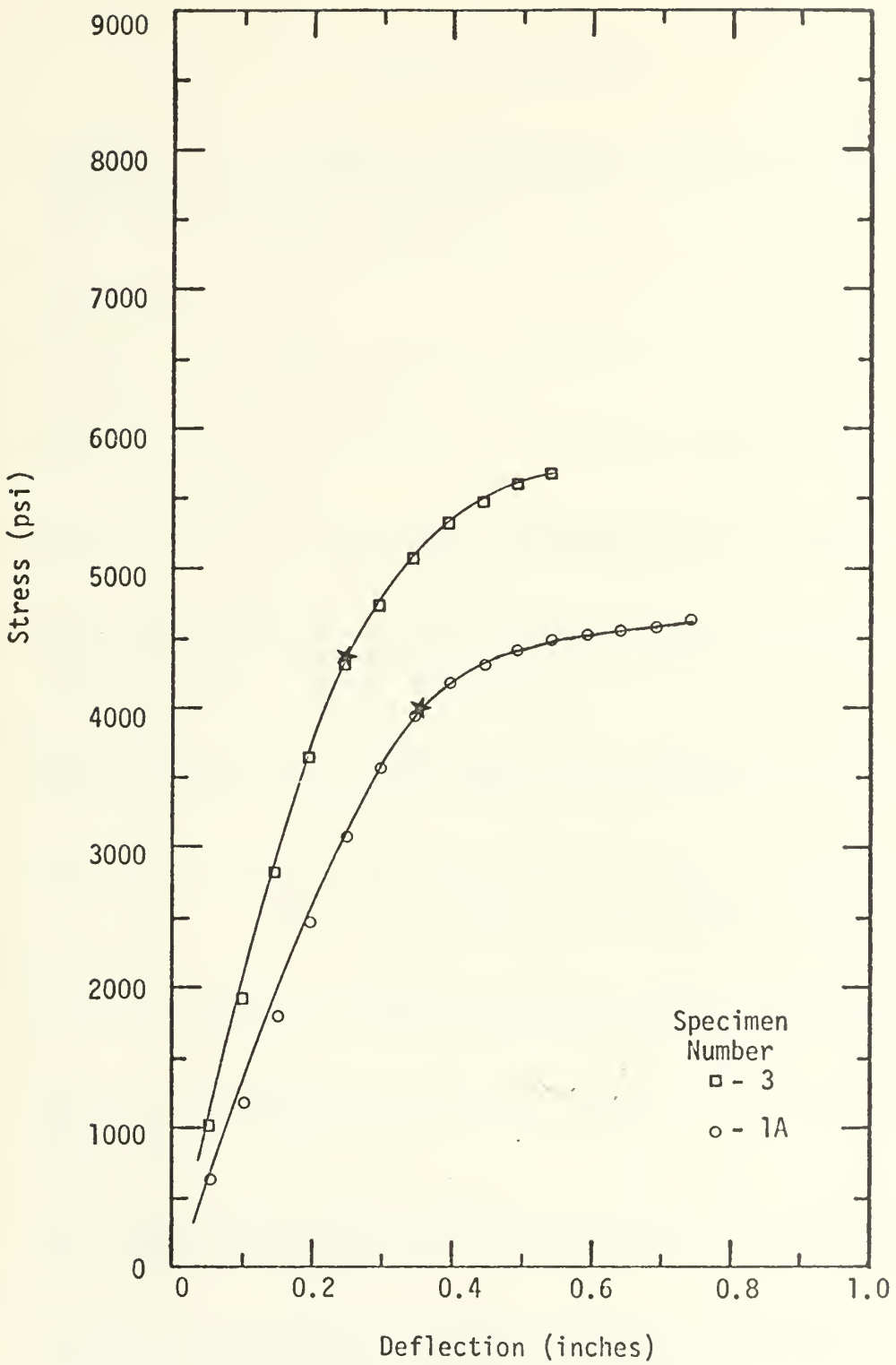

FIGURE 37. Monotonic Bending Stress vs. Deflection Plot For Panel QGL7S2

LIST OF REFERENCES

1. Simpson, M. G., Fatigue of Ferro-Cement, Master of Science (Mechanical Engineering) and Mechanical Engineer Thesis, Naval Postgraduate School, June 1974.

2. Hurd, M. K., "Ferro-Cement Boats," ACI Journal, p. 202-204, March 1969.

3. Brauer, F. E., "Ferro-Cement for Boats and Craft," Naval Engineers Journal, p. 93-105, October 1973.

4. Nervi, P. L., "Ferro-Cement: Its Characteristics and Potentialities," L'Ingegnere, V. 1, 1951.

5. Bezukladov, V. F., and others, Ship Hulls Made of Reinforced Concrete, 1968, Navships Translation No. 1148.

6. Department of the Environment (Canada), Industrial Development Branch Report No. 52, An Introduction to Design for Ferro-Cement Vessels, by G. W. Bigg, January 1972.

7. Department of the Environment (Canada), Industrial Development Branch Report No. 42, Ferro-Cement for Canadian Fishing Vessels, cimpiled and edited by W. G. Scott, August 1971.

8. Department of the Environment (Canada), Industrial Development Branch Report No. 48, Ferro-Cement for Canadian Fishing Vessels, V. 2, by A. W. Greenius and John D. Smith, January 1972.

9. Department of the Environment (Cadada), Industrial Development Branch Report No. 48, Ferro-Cement for Canadian Fishing Vessels, V. 3, prepared by The British Columbia Research Council, August 1972.

10. Naval Civil Engineering Laboratory Technical Note N-1341, Ferro-Cement Construction Panels, by H. H. Haynes and G. S. Guthrie, April 1974.

11. Naval Civil Engineering Laboratory Technical Note N-1264, Expansive Cement Concretes for Naval Construction - First Report, by J. R. Keeton, March 1973.

12. University of California (Berkeley) Report No. UC SESM 71-14, Solving the Galvanic Cell Problem in Ferro-Cement, by K. A. Christiansen and R. B. Williamson, July 1971.

13. The Society of Naval Architects and Marine Engineers Technical and Research Report No. R-14, References on Ferro-Cement in the Marine Environment, prepared by Task Group HS-6-4, October 1972.

14. Kline, S. J. and McClintock, F. A., "Describing Uncertainties in Single Sample Experiments," Mechanical Engineering, p. 3-8, January 1953.

INITIAL DISTRIBUTION LIST

		No. Copies
1.	Defense Documentation Center Cameron Station Alexandria, Virginia 22314	2
2.	Library, Code 0212 Naval Postgraduate School Monterey, California 93940	2
3.	Asst. Professor E. A. McKinnon, Code 59Mz Department of Mechanical Engineering Naval Postgraduate School Monterey, California 93940	15
4.	LT David P. Sargent, USN USS SHAKORI (ATF-162) FPO New York, New York 09501	2
5.	Harvey Haynes, Ocean Structures Division Naval Civil Engineering Laboratory Port Hueneme, California 93041	1
6.	Frank E. Brauer, Laboratory for Advanced Composites Naval Ship Research and Development Center Annapolis, Maryland 21402	1
7.	H. R. Corbin Monterey Marine, Inc. 100 Oceanview Blvd. Pacific Grove, California 93950	1
8.	Professor Tom Butler Mechanical Engineering Department U. S. Naval Academy Annapolis, Maryland 21402	1
9.	LCDR Michael G. Simpson, USN Navy Section, MAAG, Republic of China Box 12 APO San Francisco, California 96263	1
10.	Dr. Kenneth Saczalski, Code 439 Office of Naval Research 800 North Quincy Arlington, Virginia 22217	1
11.	ENS Earle Babcock SMC #2834 U. S. Naval Postgraduate School Monterey, California 93940	1

156859

Thesis
S1667 Sargent
c.1 Factors effecting the
fatigue strength of
ferro-cement.